Physica D 399 (2019) 138–152

Contents lists available at ScienceDirect

Physica D

journal homepage: www.elsevier.com/locate/physd

Stochastic neural field theory of wandering bumps on a sphere

Paul C. Bressloff

Department of Mathematics, University of Utah, Salt Lake City, UT 84112, USA

HIGHLIGHTS

- Extended theory of wandering bumps to stochastic neural fields on spheres.
- Homogeneous networks are equivariant under the action of $SO(3)$.
- Wandering is characterized by Brownian motion on the sphere for homogeneous networks.
- Weakly biased inputs suppress the effects of noise by localizing bumps.

ARTICLE INFO

Article history:
Received 3 March 2019
Received in revised form 19 April 2019
Accepted 23 April 2019
Available online 17 May 2019
Communicated by S. Coombes

Keywords:
Stochastic neural fields
Stationary bumps
Stochastic differential equations
Lie groups
$SO(3)$ symmetry
Spherical harmonics

ABSTRACT

We use a combination of group theoretic and perturbation methods to analyze the stochastic wandering of bump solutions in a neural field model on the sphere S^2. We first construct an explicit bump solution in the absence of external inputs and noise, by taking the synaptic weight distribution to be the sum of first-order spherical harmonics. The corresponding neural field equation is equivariant under the action of the special orthogonal group $SO(3)$, which implies that the bump is marginally stable with respect to rotations of the sphere. We then carry out an amplitude–phase decomposition of the solution in the presence of a weakly biased external input and weak noise, and use this to derive a pair of stochastic differential equations for the wandering of the bump, expressed in terms of angular coordinates on the sphere. The stochastic dynamics is a non-trivial generalization of the corresponding phase dynamics describing the wandering of a bump on a ring network with $SO(2)$ symmetry, since $SO(3)$ is non-abelian and S^2 is a curved manifold.

1. Introduction

There is a growing interest in studying neural field equations on compact manifolds such as the circle (or ring) S^1 and the sphere S^2. One of the first applications of a neural field model on the ring, also known as a ring attractor network, was to model the formation of population orientation tuning curves in a hypercolumn of primary visual cortex V1 [1–4]. This exploited a characteristic feature of a ring attractor network, namely, that it supports the spontaneous formation of a stationary pulse or bump, which can be established using Fourier series expansions. In the absence of external inputs, the bump is marginally stable with respect to uniform translations around the ring, reflecting the fact that the neural field equations are equivariant with respect to the action of the special orthogonal group $SO(2)$. This means that the location of the peak of the bump is arbitrary. However, a weakly biased external stimulus can lock the bump to the stimulus. From the perspective of orientation tuning, recurrent excitatory connections amplify weakly biased feedforward inputs from the thalamus in a way that is sculpted by lateral inhibitory connections, such that the tuning width and other aspects of cortical responses are primarily determined by intracortical connections rather than thalamic inputs. The output activity is said to amplify the input bias and provides a network-based encoding of the stimulus, which can be processed by upstream networks. Since the bump persists if the stimulus is removed, marginally stable neural fields on a ring have also been proposed as one mechanism for implementing a form of spatial working memory [5–11].

A natural extension of a ring attractor network on S^1 is a spherical attractor network on S^2. Carrying out an expansion in spherical harmonics, it can be established that the latter also supports stationary bump solutions, and that these can also lock to weakly biased external stimuli [12,13]. In the absence of inputs, the bumps are marginally stable with respect to rotations of the sphere, reflecting equivariance of the neural field equation with respect to the action of the special orthogonal group $SO(3)$. One major application of spherical attractor networks is to modeling the joint orientation and spatial frequency tuning of neurons in a V1 hypercolumn [12,13]. The original motivation for such a model was the observation from several optical imaging studies that both orientation and spatial frequency preferences are distributed

E-mail address: bresslof@math.utah.edu.

https://doi.org/10.1016/j.physd.2019.04.010
0167-2789/

almost continuously across cortex, with iso-orientation and iso-frequency contours being approximately orthogonal, so that they generate a local curvilinear coordinate system [14,15]. Although the existence of spatial frequency preference maps in V1 is still controversial, a more recent two-photon imaging study appears to be consistent with earlier studies [16]. Further evidence for spherical network structures in cortex has been provided by multielectrode data analysis of cortical activity patterns based on computational homology [17]. On a larger spatial scale, the Nunez model for the generation of electroencephalogram (EEG) signals [18] has recently been formulated as a neural field model on a sphere with space-dependent delays [19].

Another important consequence of an attractor neural field model operating in a marginally stable regime is that a stationary bump solution is not robust to the effects of external noise, which can illicit a stochastic wandering of the bump [7,9,20–22]. One way to investigate the stochastic wandering of bumps in neural fields is to use perturbation theory. The latter was originally applied to the analysis of traveling waves in one-dimensional neural fields [23,24], and was subsequently extended to the case of wandering bumps in single-layer and multi-layer neural fields on a ring [9,22,25–27]. The basic idea is to treat longitudinal and transverse fluctuations of a bump (or traveling wave) separately in the presence of noise, in order to take account of marginal stability. This is implemented by decomposing the stochastic neural field into a deterministic bump profile, whose spatial location or phase has a slowly diffusing component, and a small error term. (There is always a non-zero probability of large deviations from the bump solution, but these are assumed to be negligible up to some exponentially long time.) Perturbation theory can then be used to derive an explicit stochastic differential equation (SDE) for the diffusive-like wandering of the bump in the weak noise regime. (A more rigorous mathematical treatment that provides bounds on the size of transverse fluctuations has also been developed [28,29].) The wandering of bumps in a ring attractor network has also been used to model neural variability in the *in vivo* statistical responses of direction selective area-middle temporal (MT) neurons to moving gratings and plaid patterns [30]. Ponce-Alvarez et al. [30] examined the baseline levels and the evoked directional and contrast tuning of the variance of individual neurons and the noise correlations between pairs of neurons with similar direction preferences. They found experimentally that both the trial-by-trial variability and the noise correlations among MT neurons were suppressed by an external stimulus and exhibited bimodal directional tuning. Moreover, these results could be reproduced in a stochastic ring model, provided that the latter operated close to or beyond the bifurcation point for the existence of spontaneous bump solutions. A more recent analytical study based on perturbation methods has provided further insights into the underlying mechanisms of neural variability in ring attractor networks [31].

In this paper we extend the theory of wandering bumps to stochastic neural fields on the sphere. There are two features of spherical attractor networks that make such an extension non-trivial. First, in contrast to $SO(2)$, the Lie group $SO(3)$ is non-abelian and its associated Lie algebra is non-commutative. Second the sphere S^2 is a curved manifold whereas the circle S^1 is flat. Using a combination of group theory, harmonic analysis, and perturbation methods, we show how the wandering of a bump on the sphere can be characterized in terms of solutions to a pair of coupled stochastic differential equations for local coordinates on the sphere. The paper is organized as follows. In Section 2 we introduce the deterministic neural field model on a sphere, discuss the consequences of $SO(3)$ symmetry, and construct explicit stationary bump solutions using spherical harmonics. In Section 3 we turn to a stochastic version of the model and use perturbation theory to derive stochastic phase equations for the wandering of the bump on the sphere. In Section 4, we analyze these equations. First, we use the theory of stochastic processes on manifolds to show that in the absence of external inputs, the resulting phase dynamics reduces to Brownian motion on the sphere, once the curvature of S^2 is taken into account. Second, we prove that, in the absence of noise, a stationary bump can lock to a weakly-biased external input. Finally, we carry out a linear noise approximation about the stimulus-locked state to show that the localized wandering of the bump can be characterized by a pair of independent Ornstein–Uhlenbeck processes. In Appendix we summarize some basic results of Lie groups and Lie algebras, focusing on $SO(3)$. For a much more detailed introduction to Lie groups see Ref. [32], for example.

2. Neural field equation on a sphere

Let $u(\theta,\phi,t)$ denote the activity of a local population of cells on the unit sphere in $\mathbb{R}^3$ parametrized by the pair of angles $\theta\in[0,\pi]$ and $\phi\in[0,2\pi)$. The neural field equation for u is taken to be

$$\frac{\partial u(\theta,\phi,t)}{\partial t}=-u(\theta,\phi,t)+h(\theta,\phi)+\int_{\mathbf{S}^2}J(\theta,\phi|\theta',\phi')f[u(\theta',\phi',t)]\mathcal{D}(\theta',\phi') \tag{2.1}$$

where $\mathcal{D}(\theta,\phi)=\sin\theta d\theta d\phi$. Here J represents the distribution of synaptic weights from the local population at (θ',ϕ') to the local population at (θ,ϕ), $h(\theta,\phi)$ is an external input, and $f(u)$ is the smooth nonlinear firing rate function

$$f(u)=\frac{f_0}{1+\mathrm{e}^{-\eta(u-\kappa)}} \tag{2.2}$$

for constant gain η and threshold κ. Eq. (2.1) is the natural extension of the ring model to the sphere. Within the context of orientation and spatial frequency tuning in a cortical hypercolumn, see Fig. 1(a), $\phi/2\in[0,\pi)$ would represent the orientation preference and $p\in[p_{min},p_{max}]$ the spatial frequency preference of a local patch or column of cells, with p determined by θ according to the formula [12,13]

$$\theta\equiv\mathcal{Q}(p)=\pi\frac{\log(p/p_{min})}{\log(p_{max}/p_{min})} \tag{2.3}$$

Typically, the bandwidth of a hypercolumn is between three and four octaves, that is, $p_{max}\approx 2^n p_{min}$ with $n=4$. Note that, with the exception of Section 2.3, all of the analysis and results presented in the paper are independent of this particular interpretation of a neural field model on a sphere.

2.1. $SO(3)$ symmetry

Suppose that the weight distribution J is taken to be invariant with respect to coordinate rotations of the sphere, that is, the symmetry group $SO(3)$. That is, setting $z=(\theta,\phi)$, we require that for any $\gamma\in SO(3)$,

$$\gamma\cdot J(z|z')=J(\gamma^{-1}z|\gamma^{-1}z')=J(z|z').$$

(Various properties of $SO(3)$ including its action on functions on the sphere are described in Appendix.) Consider the corresponding action of $\gamma\in SO(3)$ on Eq. (2.1) for zero input $h=0$, written in the more compact form

$$\frac{\partial u(z,t)}{\partial t}=-u(z,t)+\int_{\mathbf{S}^2}J(z|z')f[u(z',t)]\mathcal{D}(z') \tag{2.4}$$

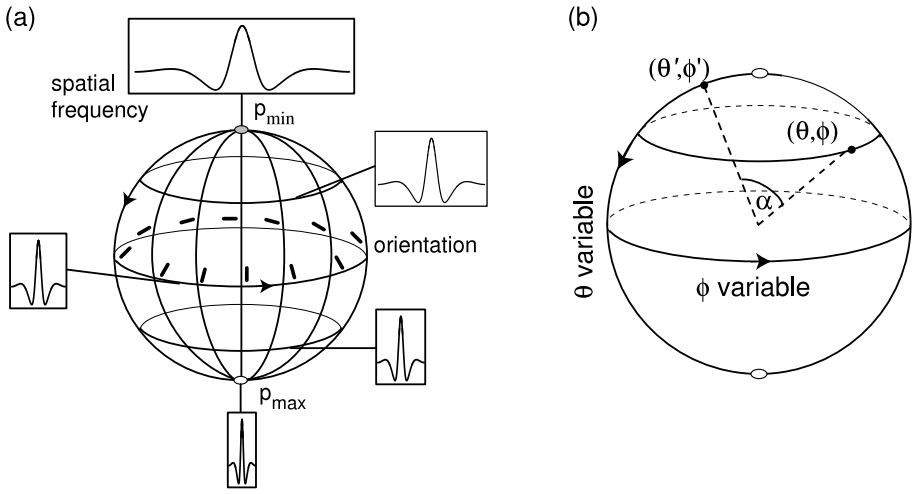

Fig. 1. Spherical network topology. Cells are labeled by the pair of angular coordinates (θ,ϕ) on the surface of a unit sphere, with $0 \le \theta < \pi$ and $0 \le \phi \le 2\pi$. (a) The angular coordinates could represent a pair of stimulus feature preferences such as spatial frequency p with $\theta = \pi \log(p/p_{min})/\log(p_{max}/p_{min})$ and orientation $\phi/2$. (b) The angular separation α of two cell populations labeled (θ,ϕ) and (θ',ϕ') along a geodesic. The $SO(3)$ invariant weight distribution (2.7) is of the form $J_0 + \bar{J}\cos\alpha$.

We have

$$\begin{aligned}\frac{\partial u(\gamma^{-1}z,t)}{\partial t} &= -u(\gamma^{-1}z,t) + \int_{S^2} J(\gamma^{-1}z|z')f[u(z',t)]Dz' \\ &= -u(\gamma^{-1}z,t) + \int_{S^2} J(z|\gamma z')f[u(z',t)]Dz' \\ &= -u(\gamma^{-1}z,t) + \int_{S^2} J(z|z'')f[u(\gamma^{-1}z'',t)]Dz''\end{aligned}$$

since $D[\gamma^{-1}z] = Dz$ and J is $SO(3)$ invariant. If we rewrite Eq. (2.4) as an operator equation, namely,

$$\mathsf{F}[u] \equiv \frac{du}{dt} - \mathsf{G}[u] = 0, \tag{2.5}$$

then it follows that $\gamma\mathsf{F}[u] = \mathsf{F}[\gamma u]$. Thus F commutes with $\gamma \in SO(3)$ and F is said to be equivariant with respect to the symmetry group $SO(3)$ [33,34].

The $SO(3)$ symmetry of the weight distribution implies that the pattern of synaptic connections depends only on the relative distance of cells on the sphere as determined by their angular separation along geodesics or great circles. That is, given two points on the sphere (θ,ϕ) and (θ',ϕ') their angular separation α is (see Fig. 1(b))

$$\cos\alpha = \cos\theta\cos\theta' + \sin\theta\sin\theta'\cos(\phi-\phi') \tag{2.6}$$

This suggests that the simplest non-trivial form for the weight distribution

$$J(\theta,\phi|\theta',\phi') = J_0 + \bar{J}\left(\cos\theta\cos\theta' + \sin\theta\sin\theta'\cos(\phi-\phi')\right) \tag{2.7}$$

Suppose that $\bar{J} > J_0$. Around the equator $(\theta,\theta' \sim \pi/2)$, we have $J \sim J_0 + \bar{J}\cos(\phi-\phi')$, which represents a Mexican hat function since cells with similar ϕ-preferences excite each other, whereas those with significantly different ϕ-preferences inhibit each other. This is the standard interaction assumption of the ring model of orientation and direction tuning [1,2]. On the other hand, around the poles $(\theta,\theta' \sim 0$ or $\theta,\theta' \sim \pi)$, all synaptic interactions are excitatory since $J \sim J_0 + \bar{J} > 0$, which is consistent with the assumption that local interactions depend on cortical separation. That is, although the cells around a pole can differ greatly in their ϕ-preference, they are physically close together on the sphere.[1]

It is possible to construct a more general form of $SO(3)$-invariant weight distribution using *spherical harmonics*. Any sufficiently smooth function $a(\theta,\phi)$ on the sphere can be expanded in a uniformly convergent double series of spherical harmonics

$$a(\theta,\phi) = \sum_{n=0}^{\infty}\sum_{m=-n}^{n} a_{nm}Y_n^m(\theta,\phi) \tag{2.8}$$

The functions $Y_n^m(\theta,\phi)$ constitute the angular part of the solutions of Laplace's equation in three dimensions, and thus form a complete orthonormal set. The orthogonality relation is

$$\int_{S^2} Y_{n_1}^{m_1*}(\theta,\phi)Y_{n_2}^{m_2}(\theta,\phi)\mathcal{D}(\theta,\phi) = \delta_{n_1,n_2}\delta_{m_1,m_2}, \tag{2.9}$$

where z^* denotes complex conjugate of z. The spherical harmonics are given explicitly by

$$Y_n^m(\theta,\phi) = (-1)^m\sqrt{\frac{2n+1}{4\pi}\frac{(n-m)!}{(n+m)!}}P_n^m(\cos\theta)e^{im\phi} \tag{2.10}$$

for $n \ge 0$ and $-n \le m \le n$, where $P_n^m(\cos\theta)$ is an associated Legendre function. Note that from properties of Legendre functions,

$$Y_n^{-m}(\theta,\phi) = (-1)^m Y_n^{m*}(\theta,\phi).$$

The action of $SO(3)$ on $Y_n^m(\theta,\phi)$ involves $(2n+1)\times(2n+1)$ unitary matrices associated with irreducible representations of $SU(2)$ [36]. From the unitarity of these representations, one can construct an $SO(3)$ invariant weight distribution of the general form

$$J(\theta,\phi|\theta',\phi') = 4\pi\sum_{n=0}^{\infty}J_n\sum_{m=-n}^{n}Y_n^{m*}(\theta',\phi')Y_n^m(\theta,\phi) \tag{2.11}$$

with J_n real. For simplicity, we will neglect higher order harmonic contributions to J by setting $J_n = 0$ for $n \ge 2$ so that Eq. (2.11) reduces to Eq. (2.7) on rescaling J_1. However, the results of this paper could be extended if a finite number of higher order harmonics were included.

[1] For simplicity, we do not explicitly distinguish between excitatory and inhibitory populations. This is a common approach to the analysis of neural fields, in which the combined effects of excitation and inhibition are incorporated using, for example, analogs of Mexican hat functions [35]. We note, however, that the methods and results presented in this paper could be extended to the case of separate excitatory and inhibitory populations, as well as different classes of interneuron.

2.2. Stationary bumps

We first construct an explicit stationary bump solution of the neural field equation (2.1) in the absence of external inputs ($h = 0$), assuming that the synaptic weight distribution is given by Eq. (2.7) with $J_0 = 0, \bar{J} > 0$.[2] Substituting $u = U(\theta, \phi)$ into Eq. (2.1) yields the integral equation

$$\begin{aligned} U(\theta,\phi) &= \bar{J}\int_{S^2}\big(\cos\theta\cos\theta' + \sin\theta\sin\theta'\cos(\phi-\phi')\big) \\ &\quad \times f(U(\theta',\phi'))\mathcal{D}(\theta',\phi') \\ &= U_x\sin\theta\cos\phi + U_y\sin\theta\sin\phi + U_z\cos\theta, \end{aligned} \tag{2.12}$$

with

$$\begin{aligned} U_x &= \bar{J}\int_{S^2}\sin\theta'\cos\phi' f(U_x\sin\theta'\cos\phi' \\ &\quad + U_y\sin\theta'\sin\phi' + U_z\cos\theta')\mathcal{D}(\theta',\phi') \end{aligned} \tag{2.13a}$$

$$\begin{aligned} U_y &= \bar{J}\int_{S^2}\sin\theta'\sin\phi' f(U_x\sin\theta'\cos\phi' \\ &\quad + U_y\sin\theta'\sin\phi' + U_z\cos\theta')\mathcal{D}(\theta',\phi') \end{aligned} \tag{2.13b}$$

$$\begin{aligned} U_z &= \bar{J}\int_{S^2}\cos\theta' f(U_x\sin\theta'\cos\phi' \\ &\quad + U_y\sin\theta'\sin\phi' + U_z\cos\theta')\mathcal{D}(\theta',\phi'). \end{aligned} \tag{2.13c}$$

We have used the trigonometric identity

$$\cos(\phi-\phi') = \cos\phi\cos\phi' + \sin\phi\sin\phi'.$$

Introducing the function

$$G(\mathbf{U}) = \bar{J}\int_{S^2} F(U_x\sin\theta'\cos\phi' + U_y\sin\theta'\sin\phi' + U_z\cos\theta')\mathcal{D}(\theta',\phi') \tag{2.14}$$

with $\mathbf{U} = (U_x, U_y, U_z)$ and $F'(u) = f(u)$, we obtain the more compact equations

$$U_x = \frac{\partial G(\mathbf{U})}{\partial U_x}, \quad U_y = \frac{\partial G(\mathbf{U})}{\partial U_y}, \quad U_z = \frac{\partial G(\mathbf{U})}{\partial U_z}. \tag{2.15}$$

First, consider the solution $U_x = U_y = 0$ and $U_z = A$. It follows from Eq. (2.13c) that the amplitude A satisfies the self-consistency condition

$$A = 2\pi\bar{J}\int_0^\pi \cos\theta'\sin\theta' f(A\cos\theta')d\theta'. \tag{2.16}$$

Existence of a bump solution reduces to the condition that Eq. (2.16) has at least one non-zero solution. We can now exploit the fact that the steady-state equation (2.4) is equivariant under the action of $SO(3)$, which implies that if $u(\theta,\phi) = A\cos\theta$ is a solution then so is $\gamma\circ u(\theta,\phi) = u(\gamma^{-1}(\theta,\phi))$ for any $\gamma \in SO(3)$. In order to determine the action of $SO(3)$ on the parameters (θ,ϕ), it is useful to treat S^2 as embedded in $\mathbb{R}^3$ with $(x,y,z) \in \mathbb{R}^3$ such that

$$x = \sin\theta\cos\phi, \quad y = \sin\theta\sin\phi, \quad z = \cos\theta. \tag{2.17}$$

This ensures $x^2+y^2+z^2 = 1$. The representation of $SO(3)$ acting on the vector space $\mathbb{R}^3$ consists of the 3×3 rotation matrices $R(\gamma)$, $\gamma \in SO(3)$, see Appendix. We can now rewrite the bump solution (2.12) in the form of a dot product, $U(\theta,\phi) = \mathbf{U}\cdot\mathbf{x}$, where $\mathbf{x} = (x,y,z)^\top$ and $\mathbf{U} = (U_x,U_y,U_z)^\top$. Equivariance can now be expressed as follows: if $\mathbf{U}\cdot\mathbf{x}$ is a solution then so is $\mathbf{U}\cdot R(\gamma)^{-1}\mathbf{x}$. However, the dot-product is invariant with respect to rotations so that $R(\gamma)\mathbf{U}\cdot\mathbf{x}$ is also a bump solution. Hence, we have a two-parameter family of bump solutions

$$U(\theta,\phi|\Theta,\Phi) = A[\cos\Theta\cos\theta + \sin\Theta\sin\theta\cos(\phi-\Phi)], \tag{2.18}$$

which represents a bump with amplitude A and a peak at $(\Theta,\Phi) \in S^2$. That is, there is a two-parameter family of bump solutions obtained by translating the bump on the surface of the sphere. Also note that each bump solution has an axis of symmetry whose direction is given by the normal to the sphere at (Θ,Φ), and

$$\gamma\circ U(\theta,\phi|\Theta,\Phi) := U(\gamma^{-1}(\theta,\phi)|\gamma^{-1}(\Theta,\Phi)) = U(\theta,\phi|\Theta,\Phi)$$

for any $\gamma \in SO(3)$.

2.3. Linear stability analysis

Linear stability of the stationary solution can be determined by considering weakly perturbed solutions of the form

$$u(\theta,\phi,t) = U(\theta,\phi|\Theta,\Phi) + \psi(\theta,\phi)e^{\lambda t}$$

for $|\psi(\theta,\phi)| \ll 1$. Substituting this expression into Eq. (2.4), Taylor expanding to first order in ψ, and imposing the stationary condition (2.12) yields the infinite-dimensional eigenvalue problem

$$\begin{aligned} \lambda\psi(\theta,\phi) &= \mathbb{L}_{\Theta,\Phi}\psi(\theta,\phi) \\ &:= -\psi(\theta,\phi) + \int_{S^2} J(\theta,\phi|\theta',\phi')f'(U(\theta',\phi'|\Theta,\Phi)) \\ &\quad \times \psi(\theta',\phi')\mathcal{D}(\theta',\phi'). \end{aligned} \tag{2.19}$$

Under the action of $\gamma \in SO(3)$ we see that

$$\begin{aligned} &\gamma\circ\mathbb{L}_{\Theta,\Phi}\psi(z) \\ &= -\psi(\gamma^{-1}z) + \int_{S^2} J(\gamma^{-1}z|z')f'(U(z'|\Theta,\Phi))\psi(z')\mathcal{D}(z') \\ &= -\psi(\gamma^{-1}z) + \int_{S^2} J(z|\gamma z')f'(U(z'|\Theta,\Phi))\psi(z')\mathcal{D}(z') \\ &= -\psi(\gamma^{-1}z) + \int_{S^2} J(z|z'')f'(U(\gamma^{-1}z''|\Theta,\Phi))\psi(\gamma^{-1}z'')\mathcal{D}(z'') \\ &= -\psi(\gamma^{-1}z) + \int_{S^2} J(z|z'')f'(U(z''|\gamma(\Theta,\Phi)))\psi(\gamma^{-1}z'')\mathcal{D}(z') \\ &= \mathbb{L}_{\gamma(\Theta,\Phi)}\gamma\circ\psi(z). \end{aligned}$$

Hence, if $\psi(\theta,\phi)$ is an eigenfunction associated with the bump $U(\theta,\phi|\Theta,\Phi)$, then $\gamma\circ\psi(\theta,\phi)$ is an eigenfunction associated with the bump $U(\theta,\phi|\gamma(\Theta,\Phi))$. Note that the eigenvalues of $\mathbb{L}_{\Theta,\Phi}$ are independent of (Θ,Φ), which reflects the fact that the stability of a bump is independent of the location of its peak. (The fact the linear operator $\mathbb{L}_{\Theta,\Phi}$ does not commute with the action of $SO(3)$ follows from the observation that a bump solution breaks $SO(3)$ symmetry. If we linearized about a uniform solution then the resulting linear operator would be $SO(3)$ equivariant.)

Eq. (2.19) can be reduced to a finite-dimensional eigenvalue problem by substituting for J using Eq. (2.7):

$$\begin{aligned} (\lambda+1)\psi(\theta,\phi) &= \mathcal{B}_x(\Theta,\Phi)\sin\theta\cos\phi \\ &\quad + \mathcal{B}_y(\Theta,\Phi)\sin\theta\sin\phi + \mathcal{B}_z(\Theta,\Phi)\cos\theta, \end{aligned} \tag{2.20}$$

where the $\mathcal{B}_j(\Theta,\Phi)$ are solutions of the self-consistency equations

$$\mathcal{B}_x = \bar{J}\int_{S^2}\sin\theta'\cos\phi' f'(U(\theta',\phi'|\Theta,\Phi))\psi(\theta',\phi')\mathcal{D}(\theta',\phi') \tag{2.21a}$$

$$\mathcal{B}_y = \bar{J}\int_{S^2}\sin\theta'\sin\phi' f'(U(\theta',\phi'|\Theta,\Phi))\psi(\theta',\phi')\mathcal{D}(\theta',\phi') \tag{2.21b}$$

[2] In our previous studies of deterministic bumps on the sphere we established the existence of bumps by considering a Heaviside or piecewise linear firing rate function [12,13].

$$\mathcal{B}_z = \bar{J}\int_{S^2} \cos\theta' f'(U(\theta',\phi'|\Theta,\Phi))\psi(\theta',\phi')\mathcal{D}(\theta',\phi'). \tag{2.21c}$$

Substituting Eq. (2.20) into (2.21) then gives the matrix equation

$$(\lambda+1)\begin{pmatrix}\mathcal{B}_x\\ \mathcal{B}_y\\ \mathcal{B}_z\end{pmatrix} = \bar{J}\mathbf{M}(\Theta,\Phi)\begin{pmatrix}\mathcal{B}_x\\ \mathcal{B}_y\\ \mathcal{B}_z\end{pmatrix}, \tag{2.22}$$

where

$$\mathbf{M} = \begin{pmatrix} \mathcal{I}[\sin^2\theta\cos^2\phi] & \mathcal{I}[\sin^2\theta\cos\phi\sin\phi] & \mathcal{I}[\sin\theta\cos\theta\cos\phi] \\ \mathcal{I}[\sin^2\theta\cos\phi\sin\phi] & \mathcal{I}[\sin^2\theta\sin^2\phi] & \mathcal{I}[\sin\theta\cos\theta\sin\phi] \\ \mathcal{I}[\sin\theta\cos\theta\cos\phi] & \mathcal{I}[\sin\theta\cos\theta\sin\phi] & \mathcal{I}[\cos^2\theta] \end{pmatrix} \tag{2.23}$$

and, for any product $v(\theta)u(\phi)$,

$$\mathcal{I}[v(\theta)u(\phi)] = \int_{S^2} v(\theta)u(\phi)f'(U(\theta,\phi|\Theta,\Phi))\mathcal{D}(\theta,\phi). \tag{2.24}$$

(For notational simplicity, we have suppressed the dependence of $\mathcal{I}$ on (Θ,Φ).)

Given the fact that the eigenvalues are independent of the location of the peak of the bump, we set $(\Theta,\Phi) = (0,0)$ in Eq. (2.22) so that $\mathcal{I}\to\mathcal{I}_0$ with

$$\mathcal{I}_0[v(\theta)u(\phi)] = \int_0^\pi v(\theta)\sin\theta f'(A\cos(\theta))d\theta \int_0^{2\pi} u(\phi)d\phi. \tag{2.25}$$

It immediately follows that

$$\mathcal{I}_0[\sin\theta\cos\theta\sin\phi] = \mathcal{I}_0[\sin\theta\cos\theta\cos\phi] = \mathcal{I}_0[\sin^2\theta\cos\phi\sin\phi] = 0,$$

and

$$\mathcal{I}_0[\sin^2\theta\cos^2\phi] = \mathcal{I}_0[\sin^2\theta\sin^2\phi] = \frac{1}{2}\mathcal{I}_0[\sin^2\theta].$$

Integrating equation (2.16) by parts implies that

$$A = \frac{\pi\bar{J}}{2}(f(A)-f(-A)) - \frac{\pi\bar{J}A}{2}\int_0^\pi (1-2\sin^2\theta)\sin\theta f'(A\cos\theta)d\theta = \frac{A\bar{J}}{2}\mathcal{I}_0[\sin^2\theta],$$

so that

$$\mathcal{I}_0[\sin^2\theta] = 2/\bar{J}.$$

Finally, exploiting the fact that $\mathcal{I}_0$ is a linear functional of v, we have

$$\mathcal{I}_0[\cos^2\theta] = \mathcal{I}_0[1-\sin^2\theta] = \mathcal{I}_0[1] - \mathcal{I}[\sin^2\theta] = \mathcal{I}_0[1] - 2/\bar{J}.$$

Combining these results, Eq. (2.22) reduces to

$$(\lambda+1)\begin{pmatrix}\mathcal{B}_x(0.0)\\ \mathcal{B}_y(0,0)\\ \mathcal{B}_z(0,0)\end{pmatrix} = \begin{pmatrix}1&0&0\\0&1&0\\0&0&\bar{J}\mathcal{I}_0[1]-2\end{pmatrix}\begin{pmatrix}\mathcal{B}_x(0,0)\\ \mathcal{B}_y(0,0)\\ \mathcal{B}_z(0,0)\end{pmatrix}. \tag{2.26}$$

It follows that there is a doubly-degenerate zero eigenvalue $\lambda_{1,2} = 0$ with corresponding eigenvectors $\mathbf{e}_1 = (1,0,0)^\top$ and $\mathbf{e}_2 = (0,1,0)^\top$, and a simple non-zero eigenvalue

$$\lambda_3 = 2\pi\bar{J}\int_0^\pi \sin\theta f'(A\cos(\theta))d\theta - 3 \tag{2.27}$$

$$= -\frac{2\pi\bar{J}}{A}\int_0^\pi \frac{d}{d\theta}f(A\cos(\theta))d\theta - 3 \tag{2.28}$$

$$= \frac{2\pi\bar{J}}{A}[f(A)-f(-A)] - 3. \tag{2.29}$$

with corresponding eigenvector $\mathbf{e}_3 = (0,0,1)^\top$. Thus linear stability of the bump reduces to the condition $\lambda_3 < 0$. (Note that there also exist infinitely many eigenvalues that are equal to -1, which are associated with higher order spherical harmonics and form the essential spectrum. However, since they lie in the left-half complex λ-plane, they do not affect stability.) The existence of a pair of zero eigenvalues is a consequence of the fact that the neural field equation (2.4) is equivariant with respect to the action of $SO(3)$, and would hold for any weight function of the form (2.11).

Given the eigenvectors for $(\Theta,\Phi) = 0$ we can determine the corresponding eigenvectors at a general bump location (Θ,Φ) using $SO(3)$ symmetry. Applying the $\mathbb{R}^3$ embedding (2.17), the eigenvalue equation (2.20) can be rewritten as

$$(\lambda+1)\hat{\psi}(\mathbf{x}|\Theta,\Phi) = \mathbf{B}(\Theta,\Phi)\cdot\mathbf{x},$$

with $\mathbf{x} = (x,y,z) \in \mathbb{R}^3$ a point on the unit sphere, $\hat{\psi}(\mathbf{x}) = \psi(\theta,\phi)$, and $\mathbf{B} = (\mathcal{B}_x,\mathcal{B}_y,\mathcal{B}_z)^\top \in \mathbb{R}^3$. There is an induced $SO(3)$ action on the vector $\mathbf{B}$, consisting of rotations that preserve the norm $\mathcal{B}_x^2+\mathcal{B}_y^2+\mathcal{B}_z^2$. That is,

$$\begin{aligned}(\lambda+1)\hat{\psi}(R(\gamma)^{-1}\mathbf{x}|\Theta,\Phi) &= \mathbf{B}(\Theta,\Phi)\cdot R(\gamma)^{-1}\mathbf{x}\\ &= R(\gamma)\mathbf{B}(\Theta,\Phi)\cdot\mathbf{x},\\ &= \mathbf{B}(\gamma(\Theta,\Phi))\cdot\mathbf{x},\end{aligned}$$

where $R(\gamma)$ is the 3×3 rotation matrix corresponding to $\gamma \in SO(3)$. Now note that the point $(0,0)\in S^2$ can be mapped to an arbitrary point $(\Theta,\Phi)\in S^2$ by first rotating about the y-axis by Θ and then rotating about the z-axis by Φ, see Fig. 2(a). The net rotation matrix is

$$R(\Theta,\Phi) = R_3(\Phi)R_2(\Theta).$$

(We could use any sequence of rotations that map the north pole to the point (Θ,Φ) on the sphere. Another simple example is $R(\Theta,\Phi) = R_3(\Phi-\pi/2)R_1(-\Theta)$, see Fig. 2(b).) It follows that the unique vector $\mathbf{B}_3(\Theta,\Phi)$ corresponding to the eigenvalue λ_3 is

$$\mathbf{B}_3(\Theta,\Phi) = R(\Theta,\Phi)\mathrm{e}_3,$$

whereas the two-dimensional vector eigenspace for the degenerate zero eigenvalue is spanned by the vectors

$$\mathbf{B}_r(\Theta,\Phi) = R(\Theta,\Phi)\mathrm{e}_r, \quad r=1,2.$$

2.4. Marginal stability

The existence of a pair of zero eigenvalues is a consequence of the fact that the bump solution is marginally stable with respect to rotations of the sphere. In order to understand this more deeply, consider the time-independent version of Eq. (2.4),

$$U(z) = \int_{S^2} J(z|z')f(U(z'))Dz'. \tag{2.30}$$

Since J is invariant with respect to the action of $SO(3)$, we have

$$\gamma\circ U(z) = \int_{S^2} J(z|z')f(\gamma\circ U(z'))Dz'.$$

Now suppose that γ is in a neighborhood of the identity element so that we can write (see Appendix)

$$\gamma\circ U(\theta,\phi) = U(\theta,\phi) + \sum_{j=1}^3 \varphi_j X_j U(\theta,\phi), \tag{2.31}$$

for $|\varphi_j| \ll 1$ and the X_j are the generators of the associated Lie algebra,

$$X_1 = \sin\phi\frac{\partial}{\partial\theta} + \frac{\cos\theta\cos\phi}{\sin\theta}\frac{\partial}{\partial\phi},$$
$$X_2 = \cos\phi\frac{\partial}{\partial\theta} - \frac{\cos\theta\sin\phi}{\sin\theta}\frac{\partial}{\partial\phi}, \quad X_3 = \frac{\partial}{\partial\phi}. \tag{2.32}$$

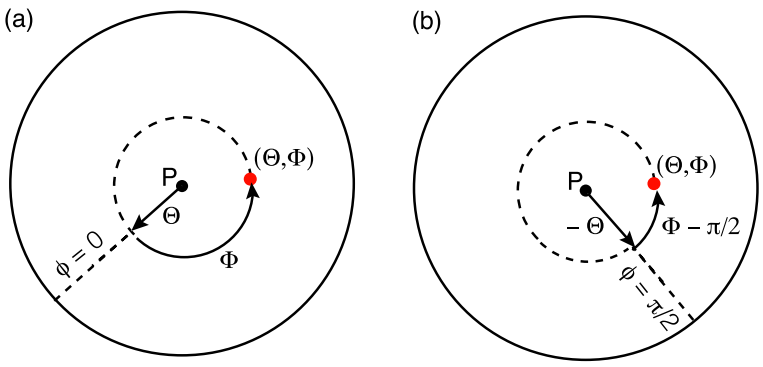

Fig. 2. Schematic illustration of two different sequences of rotations that map the north pole P to an arbitrary point (Θ, Φ) on the sphere. The sphere is viewed from above. (a) Rotation by Θ along the great circle $\phi = 0$ followed by a rotation Φ about the z-axis. (b) Rotation by $-\Theta$ about the great circle $\phi = \pi/2$ followed by a rotation $\Phi - \pi/2$ about the z-axis.

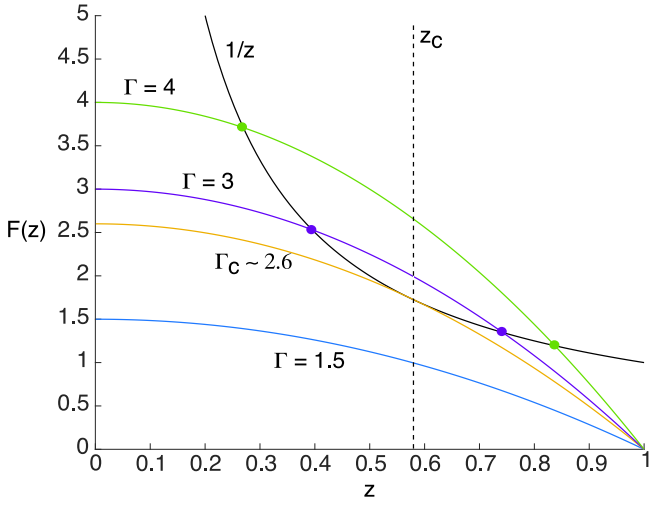

Fig. 3. Graphical solution of the bump amplitude equation (2.16) for a Heaviside firing rate function. The function $F(z) = \Gamma(1 - z^2)$ is plotted for various values of Γ. Bump solutions correspond to intercepts of $F(z)$ with the curve $y = 1/z$. As $\Gamma = \pi\bar{J}/\kappa$ is increased, a saddle–node bifurcation occurs, resulting in the emergence of a pair of stationary bumps, a small amplitude unstable bump and a large amplitude (marginally) stable bump.

Substituting into the transformed steady-state equation (2.31) and keeping terms first order in φ_j yields

$$\sum_{j=1}^{3} \varphi_j X_j U(z) = \int_{S^2} J(z|z') f'(U(z')) \sum_{j=1}^{3} \varphi_j X_j U(z') Dz'. \tag{2.33}$$

Comparison with the eigenvalue equation (2.19) suggests that the eigenfunctions $\psi_j(\theta, \phi|\Theta, \Phi) = X_j U(\theta, \phi|\Theta, \Phi)$, $j = 1, 2, 3$, lie in the null space of the linear operator $\mathbb{L}_{\Theta,\Phi}$. At first sight, this seems to contradict the fact that the marginally stable manifold is two-dimensional. However, there are only two linearly independent functions in the set $\{\psi_1, \psi_2, \psi_3\}$. This follows from the fact that the bump solution has an axis of symmetry. For example, if $U(\theta, \phi) = A\cos\theta$, then the axis of symmetry is the z-axis and $\psi_3 = X_3 U = 0$.

2.5. Explicit results for a Heaviside firing rate function

The above analysis can be further simplified by taking the infinite gain limit $\gamma \to \infty$ of the sigmoid firing rate function (2.2), which becomes a Heaviside function (for $f_0 = 1$):

$$f(u) = H(u - \kappa) = \begin{cases} 0 & u < \kappa \\ 1 & u \geq \kappa \end{cases} \tag{2.34}$$

Let us first consider the self-consistency condition (2.16) for the amplitude A of a deterministic bump solution. Since $U(\theta) = A\cos\theta$ is a monotonically decreasing function of θ on $[0, \pi]$, it will cross the threshold κ at a single location $\theta = a \in (0, \pi)$, with

$$a = \cos^{-1}\frac{\kappa}{A}$$

and $A \geq \kappa$. Eq. (2.16) thus becomes

$$\begin{aligned} A &= 2\pi\bar{J}\int_0^{\cos^{-1}\kappa/A} \cos\theta' \sin\theta' d\theta' = \pi\bar{J}\int_0^{\cos^{-1}\kappa/A} \sin 2\theta' d\theta' \\ &= \frac{\pi\bar{J}}{2}\left[1 - \cos 2\left(\cos^{-1}\kappa/A\right)\right] = \pi\bar{J}\left[1 - \cos^2\left(\cos^{-1}\kappa/A\right)\right] \\ &= \pi\bar{J}\left[1 - \left(\frac{\kappa}{A}\right)^2\right] \end{aligned}$$

Setting $z = \kappa/A$, we have the equation

$$z^{-1} = \Gamma(1 - z^2), \quad \Gamma = \frac{\pi\bar{J}}{\kappa}.$$

Using a graphical construction, it follows that for $\Gamma > \Gamma_c$ for some critical parameter Γ_c there exists a pair of bump solutions, see Fig. 3. Imposing the additional condition $1 = 2\Gamma z^3$ at the critical point shows that $\Gamma_c \approx 2.598$ and $z_c = 1/\sqrt{3}$. Stability of the bumps is determined by the sign of the eigenvalue λ_3 of Eq. (2.29). In the case of a Heaviside function, we have

$$\lambda_3 = \frac{2\pi\bar{J}}{A}[H(A - \kappa) - H(-A - \kappa)] - 3 = \frac{2\Gamma\kappa}{A} - 3. \tag{2.35}$$

Denoting a solution to the equation $z^{-1} = \Gamma(1 - z^2)$ by $z = z^*$, it follows that the bump is stable if $(1 - z^{*2}) > 2/3$, that is, if $z^* < z_c = 1/\sqrt{3}$. It can be seen from Fig. 3 that for $\Gamma > \Gamma_c$ the larger amplitude bump is stable, whereas the smaller amplitude bump is unstable. (For smaller gains, one typically finds that the uniform state is unstable and there exists a single stable bump.)

2.6. Weakly biased external input

Marginal stability of the neural field equation (2.1) in the absence of an external input ($h = 0$) has a number of important consequences. First, the presence of a weakly biased external stimulus can lock the bump to the stimulus. The output activity is said to amplify the input bias and provides a network-based encoding of the stimulus, which can be processed by upstream

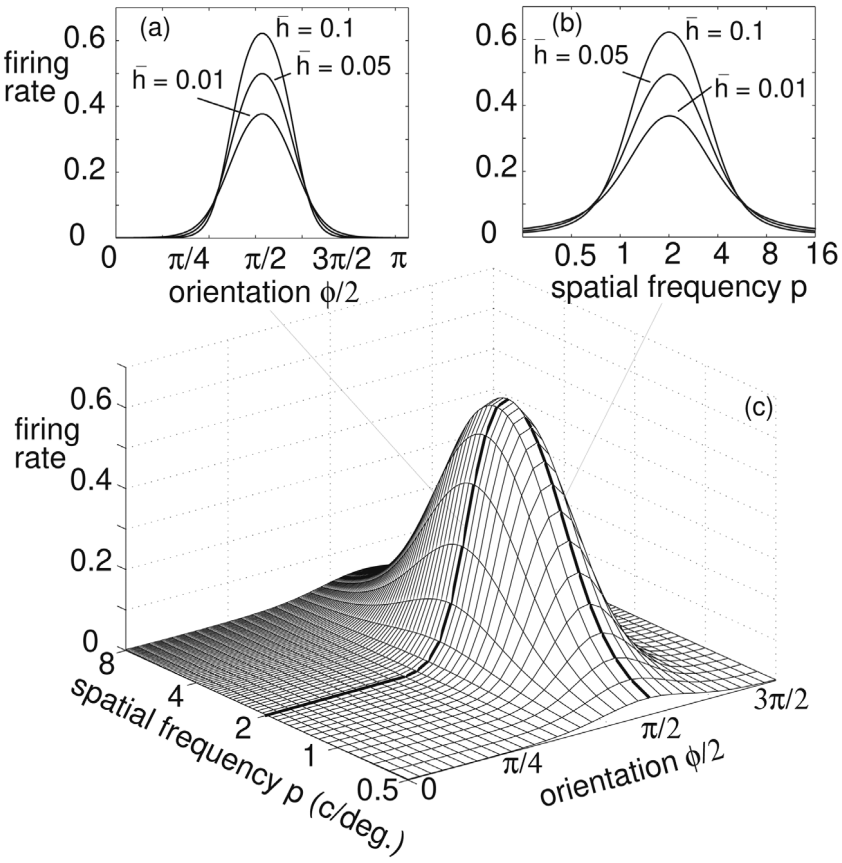

Fig. 4. Plot of normalized firing rate $f(u)/f_0$ in response to a weakly biased input from, with $\bar{\theta} = \pi/2$, $\bar{\phi} = \pi$ and $\bar{h} \ll 1$. The firing rate function has a gain $\eta = 5$, and a threshold $\kappa = 0.6$. The weight coefficients in Eq. (2.11) are $J_0 = -2, J_1 = 1$ and $J_n = 0$ for $n > 1$. (a) and (b) Spatial frequency and orientation tuning curves. (c) Tuning surface in the $\{p, \phi\}$ plane.

networks. For the sake of illustration, consider an external input of the form

$$h(\theta, \phi|\bar{\theta}, \bar{\phi}) = h_0 + \bar{h}\left(\cos\bar{\theta}\cos\theta + \sin\bar{\theta}\sin\theta\cos(\phi - \bar{\phi})\right). \quad (2.36)$$

This represents a unimodal function on the sphere with a single peak at $(\bar{\theta}, \bar{\phi})$, which breaks the $SO(3)$ symmetry of the homogeneous neural field. Here h_0 is a background constant input, which can be set to zero by an appropriate uniform shift in u and the threshold κ. The constant $\bar{h}$ measures the degree of bias. The response of a spherical attractor network to weakly-biased inputs has been covered extensively elsewhere in terms of orientation and spatial frequency tuning in cortical hypercolumns [12,13]. In Fig. 4 we show one example plot of a stationary bump solution in response to a weakly biased input with a peak at $\bar{\theta} = \pi/2$ and $\bar{\phi} = \pi$. Fig. 4(a) shows a surface plot in the $\{p, \phi\}$-plane for $\bar{h} = 0.1$ with p related to θ according to Eq. (2.3). It can be seen that the network exhibits a tuning surface that is localized with respect to two-dimensional spatial frequency and its peak is locked to the input at $\bar{p} = 2$ cycles/deg, $\bar{\phi} = \pi$. In Fig. 4(b) we plot the response as a function of spatial frequency at the optimal orientation for various input amplitudes $\bar{h}$. The height of the spatial frequency tuning curves increases with the input amplitude $\bar{h}$ but the width at half-height is approximately the same (as can be checked by rescaling the tuning curves to the same height). Since $\bar{h}$ increases with the contrast of a stimulus, this shows that the network naturally exhibits contrast–invariance. Corresponding orientation tuning curves are shown in Fig. 4(c), and are also found to exhibit contrast–invariance. Note that projecting the spherical tuning surface onto the $\{p, \phi\}$-plane breaks the underlying $SO(3)$ symmetry of the sphere. Consequently, the shape of the planar tuning surface is not invariant under shifts in the location of the peak of the tuning surface, which is consistent with experimental observations [13].

3. Stochastic spherical model

A second consequence of marginal stability is that a stationary bump is not robust to the effects of external noise, which can elicit a stochastic wandering of the bump over the surface of the sphere. An analogous phenomenon has been studied extensively in the case of neural fields on a line and on a ring using perturbation methods [9,22–24,26,27], variational principles [28,29] and stochastic analysis [37,38]. As highlighted in the introduction, it is necessary to treat longitudinal and transverse fluctuations of a one-dimensional bump separately in the presence of noise. This is achieved by decomposing the stochastic neural field into a deterministic bump profile, whose spatial location or phase has a slowly diffusing component, and a small error term. This yields an explicit stochastic differential equation (SDE) for the diffusive-like wandering of the bump in the weak noise regime. In this section we will extend perturbation theory to analyze the stochastic wandering of a bump in a stochastic neural field on the sphere.

We begin by introducing a stochastic version of Eq. (2.1) according to

$$du(\theta, \phi, t) = \Big[-u(\theta, \phi, t) + \int_{S^2} J(\theta, \phi|\theta', \phi') f(u(\theta', \phi', t)) \mathcal{D}(\theta', \phi') + \sqrt{\epsilon} h(\theta, \phi) \Big] dt + \sqrt{2\epsilon} dW(\theta, \phi, t), \quad (3.1)$$

where the synaptic weight distribution is given by Eq. (2.7) and the external input $h(\theta,\phi) = h(\theta,\phi|\bar{\theta},\bar{\phi})$ is given by Eq. (2.36) with $J_0 = h_0 = 0$. The final term on the right-hand side of Eq. (3.1) represents external additive noise. In particular, we will take W to be a Q-wiener process that takes values in $L^2(S^2)$ and is isotropic in space. It follows that W can be characterized by a Karhunen–Loeve expansion in spherical harmonics [39]. For concreteness, we will take this to be a finite sum of the form

$$W(\theta,\phi,t) = \sum_{n=0}^{K} \sqrt{C_n}\Big[A_n^0(t)Y_n^0(\theta,\phi) + \sum_{m\neq 0}[A_n^m(t)Y_n^m(\theta,\phi) + A_n^{m*}(t)Y_n^{m*}(\theta,\phi)]\Big], \tag{3.2}$$

where $A_n^m = W_n^m + i\widehat{W}_n^m$ with $W_n^m(t)$ and $\widehat{W}_n^m(t)$ independent Wiener processes,

$$\begin{aligned}
&\mathbb{E}[dW_n^m] = \mathbb{E}[d\widehat{W}_n^m] = 0,\\
&\mathbb{E}[dW_n^m(t)dW_{n'}^{m'}(t')] = \delta_{n,n'}\delta_{m,m'}\delta(t-t')dt\,dt',\\
&\mathbb{E}[d\widehat{W}_n^m(t)d\widehat{W}_{n'}^{m'}(t')] = \delta_{n,n'}\delta_{m,m'}\delta(t-t')dt\,dt',\\
&\mathbb{E}[dW_n^m(t)d\widehat{W}_{n'}^{m'}(t')] = 0,
\end{aligned} \tag{3.3}$$

and $\delta(t)$ is the Dirac delta function. It follows that

$$\begin{aligned}
&\mathbb{E}[dW(\theta,\phi,t)] = 0,\\
&\mathbb{E}[dW(\theta,\phi,t)dW(\theta',\phi',t')] = C(\theta,\phi|\theta',\phi')\delta(t-t')dt\,dt',
\end{aligned} \tag{3.4}$$

where

$$C(\theta,\phi|\theta',\phi') = \sum_{n=0}^{K} C_n \sum_{m=-n}^{n} Y_n^{m*}(\theta,\phi)Y_n^m(\theta',\phi'). \tag{3.5}$$

Under the assumed form of the noise, the correlation function C is $SO(3)$ invariant. Finally, note that in order to use perturbation methods, we have scaled the noise and the external stimulus in Eq. (3.1) by the constant factor $\sqrt{\epsilon}$ with $0 < \epsilon \ll 1$.

Motivated by previous studies of wandering bumps in stochastic neural fields on rings, we introduce the amplitude–phase decomposition [9,23]

$$u(\theta,\phi,t) = U(\theta,\phi|\Theta(t),\Phi(t)) + \sqrt{\epsilon}v(\theta,\phi,t), \tag{3.6}$$

with U given by the bump solution (2.18). As it stands, this decomposition is non-unique, unless an additional mathematical constraint is imposed that can define $\Theta(t)$, $\Phi(t)$, and $v(\theta,\phi,t)$ uniquely. Within the context of formal perturbation methods, this is achieved by imposing a solvability condition that ensures that the error term can be identified with fast transverse fluctuations, which converge to zero exponentially in the absence of noise.[3]

3.1. Perturbation analysis

Suppose that $v \in L^2(S^2)$, that is,

$$\|v\|^2 = \langle v, v\rangle = \int_{S^2} v(\theta,\phi)^2\mathcal{D}(\theta,\phi) < \infty.$$

Substituting the decomposition (3.6) into the stochastic neural field equation (3.1)

$$\begin{aligned}
&\partial_\Theta U(\theta,\phi|\Theta,\Phi)d\Theta + \partial_\Phi U(\theta,\phi|\Theta,\Phi)d\Phi\\
&\quad + O(d\Theta^2, d\Phi^2, d\Theta\,d\Phi) + \sqrt{\epsilon}dv(\theta,\phi,t)\\
&= \big[-U(\theta,\phi|\Theta,\Phi) - \sqrt{\epsilon}v(\theta,\phi,t) + \sqrt{\epsilon}h(\theta,\phi)\big]dt\\
&\quad + \sqrt{2\epsilon}dW(\theta,\phi,t)\\
&\quad + \int_{S^2} J(\theta,\phi|\theta',\phi')f\big(U(\theta',\phi'|\Theta,\Phi) + \sqrt{\epsilon}v(\theta',\phi',t)\big)\\
&\quad \times \mathcal{D}(\theta',\phi')dt.
\end{aligned} \tag{3.7}$$

The $O(d\Theta^2, d\Phi^2, d\Theta\,d\Phi)$ terms are a consequence of Ito's lemma. They turn out to be $O(\epsilon)$ and can thus be ignored to leading order in the presence of an external input. (They will play an important role in the absence of an input, see Section 4.) Introduce the series expansion $v = v_0 + \sqrt{\epsilon}v_1 + O(\epsilon)$, Taylor expand the nonlinear function f, impose the stationary solution (2.12), and drop all $O(\epsilon)$ terms. This gives, after dropping the zero index on v_0,

$$\begin{aligned}
\sqrt{\epsilon}dv(\theta,\phi,t) &= \sqrt{\epsilon}\mathbb{L}_{\Theta,\Phi}v(\theta,\phi,t)dt\\
&\quad + \sqrt{\epsilon}h(\theta,\phi)dt + \sqrt{2\epsilon}dW(\theta,\phi,t),\\
&\quad -\partial_\Theta U(\theta,\phi|\Theta,\Phi)d\Theta - \partial_\Phi U(\theta,\phi|\Theta,\Phi)d\Phi,
\end{aligned} \tag{3.8}$$

where $\mathbb{L}_{\Theta,\Phi}$ is the linear operator defined in Eq. (2.19). In particular, $\mathbb{L}_{\Theta,\Phi}$ has a 2D null space spanned by the linearly-dependent set $\{X_jU, j = 1,2,3\}$. For example, for $\mathbb{L}_{0,0}$ the null space is $\{\cos\phi\sin\theta, \sin\phi\sin\theta\}$, see Section 2.3. This then implies a pair of solvability conditions for the existence of bounded solutions of Eq. (3.8), namely, that dv is orthogonal to all elements of the null space of the adjoint operator $\mathbb{L}^\dagger_{\Theta,\Phi}$. The corresponding adjoint operator is

$$\begin{aligned}
\mathbb{L}^\dagger_{\Theta,\Phi}v(\theta,\phi) &= -v(\theta,\phi)\\
&\quad + f'(U(\theta,\phi|\Theta,\Phi))\int_{S^2} J(\theta,\phi|\theta',\phi')v(\theta',\phi')\mathcal{D}(\theta',\phi').
\end{aligned} \tag{3.9}$$

We have used the fact that $J(\theta,\phi|\theta',\phi') = J(\theta',\phi'|\theta,\phi)$.

Let $\mathcal{V}_r(\theta,\phi|\Theta,\Phi)$, $r = 1,2$, span the 2D adjoint null space of $\mathbb{L}^\dagger_{\Theta,\Phi}$. Now taking the inner product of both sides of Eq. (3.8) with respect to $\mathcal{V}_r$ and using $SO(3)$ symmetry then yields the following SDE to leading order:

$$\Gamma_r d\Theta + \Lambda_r d\Phi = \sqrt{\epsilon}H_r(\Theta,\Phi)dt + \sqrt{2\epsilon}dW_r(t), \quad r = 1,2, \tag{3.10}$$

where

$$H_r(\Theta,\Phi) = \int_{S^2} \mathcal{V}_r(\theta,\phi|\Theta,\Phi)h(\theta,\phi|\bar{\theta},\bar{\phi})\mathcal{D}(\theta,\phi), \tag{3.11a}$$

$$\Gamma_r = \int_{S^2} \mathcal{V}_r(\theta,\phi|\Theta,\Phi)\partial_\Theta U(\theta,\phi|\Theta,\Phi)\mathcal{D}(\theta,\phi), \tag{3.11b}$$

$$\Lambda_r = \int_{S^2} \mathcal{V}_r(\theta,\phi|\Theta,\Phi)\partial_\Phi U(\theta,\phi|\Theta,\Phi)\mathcal{D}(\theta,\phi), \tag{3.11c}$$

$$W_r(t) = \int_{S^2} \mathcal{V}_r(\theta,\phi|\Theta,\Phi)W(\theta,\phi,t)\mathcal{D}(\theta,\phi). \tag{3.11d}$$

Eqs. (3.11d) imply that $\mathbb{E}[dW_r(\Theta,\Phi,t)] = 0$ and

$$\mathbb{E}[dW_r(t)dW_s(t')] = D_{rs}\delta(t-t')dt'dt,$$

with

$$\begin{aligned}
D_{rs} &= \int_{S^2}\int_{S^2} \mathcal{V}_r(\theta,\phi|\Theta,\Phi)\mathcal{V}_s(\theta',\phi'|\Theta,\Phi)C(\theta,\phi|\theta',\phi')\mathcal{D}(\theta,\phi)\\
&\quad \times \mathcal{D}(\theta',\phi').
\end{aligned} \tag{3.12}$$

3.2. Evaluation of H_r, Γ_r, Λ_r and D_{rs}

In order to determine the functions in Eq. (3.11), we need to obtain explicit expressions for the null vectors $\mathcal{V}_r$. The latter are solutions to the equation

$$\mathcal{V}(\theta,\phi) = f'(U(\theta,\phi|\Theta,\Phi))\int_{S^2} J(\theta,\phi|\theta',\phi')\mathcal{V}(\theta',\phi')\mathcal{D}(\theta',\phi') \tag{3.13}$$

[3] Note that $(\Theta(t),\Phi(t))$ denote the stochastic coordinates of the peak of the bump U in the decomposition (3.6), whereas (θ,ϕ) are the coordinates of the random fields on the sphere. That is, $(\Theta(t),\Phi(t))$ are not a stochastic version of deterministic variables $(\theta(t),\phi(t))$.

Substituting for J using Eq. (2.7) with $J_0 = 0$, we see that

$$\mathcal{V}(\theta,\phi) = f'(U(\theta,\phi|\Theta,\Phi))[V_x \sin\theta\cos\phi + V_y \sin\theta\sin\phi + V_z\cos\theta]$$

with

$$V_x = \bar{J}\int_{S^2} \sin\theta'\cos\phi'\mathcal{V}(\theta',\phi')\mathcal{D}(\theta',\phi') \tag{3.14a}$$

$$V_y = \bar{J}\int_{S^2} \sin\theta'\sin\phi'\mathcal{V}(\theta',\phi')\mathcal{D}(\theta',\phi') \tag{3.14b}$$

$$V_z = \bar{J}\int_{S^2} \cos\theta'\mathcal{V}(\theta',\phi')\mathcal{D}(\theta',\phi'). \tag{3.14c}$$

Substituting the expression for $\mathcal{V}(\theta,\phi)$ into the right-hand side of Eqs. (3.14) then leads to a matrix equation of the form (2.26) with $\lambda = 0$:

$$\begin{pmatrix} V_x \\ V_y \\ V_z \end{pmatrix} = \bar{J}\mathbf{M}(\Theta,\Phi)\begin{pmatrix} V_x \\ V_y \\ V_z \end{pmatrix}, \tag{3.15}$$

with the matrix $\mathbf{M}$ given by Eq. (2.23). Recall from Section 2.2, that the matrix $\bar{J}\mathbf{M}(\Theta,\Phi) - \mathbf{I}$ has a two-dimensional null-space, which we take to be spanned by the vectors $\mathbf{v}_r(\Theta,\Phi)$, $r = 1, 2$. We conclude that the adjoint null space of $\mathbb{L}^\dagger_{\Theta,\Phi}$ is spanned by

$$\begin{aligned}\mathcal{V}_r(\theta,\phi|\Theta,\Phi) &= f'(U(\theta,\phi|\Theta,\Phi)) \\ &\times [v_{r,x}(\Theta,\Phi)\sin\theta\cos\phi + v_{r,y}(\Theta,\Phi)\sin\theta\sin\phi \\ &+ v_{r,z}(\Theta,\Phi)\cos\theta],\end{aligned} \tag{3.16}$$

with $v_{r,x}^2 + v_{r,y}^2 + v_{r,z}^2 = 1$. In particular,

$$\begin{aligned}\mathcal{V}_1(\theta,\phi|0,0) &= f'(A\cos\theta)\sin\theta\cos\phi, \\ \mathcal{V}_2(\theta,\phi|0,0) &= f'(A\cos\theta)\sin\theta\sin\phi,\end{aligned} \tag{3.17}$$

and

$$\mathbf{v}_1(\Theta,\Phi) = R(\Theta,\Phi)\mathrm{e}_1, \quad \mathbf{v}_2(\Theta,\Phi) = R(\Theta,\Phi)\mathrm{e}_2. \tag{3.18}$$

Hence, we find explicitly that

$$\begin{aligned}\mathcal{V}_1(\theta,\phi|\Theta,\Phi) &= f'(U(\theta,\phi|\Theta,\Phi))[\cos\Theta\sin\theta\cos(\phi-\Phi) \\ &\quad - \sin\Theta\cos\theta] \\ &= A^{-1}f'(U(\theta,\phi|\Theta,\Phi))\partial_\Theta U(\theta,\phi|\Theta,\Phi) \\ &= A^{-1}\partial_\Theta f(U(\theta,\phi|\Theta,\Phi))\end{aligned} \tag{3.19a}$$

$$\begin{aligned}\mathcal{V}_2(\theta,\phi|\Theta,\Phi) &= f'(U(\theta,\phi|\Theta,\Phi))\sin\theta\sin(\phi-\Phi) \\ &= A^{-1}(\sin\Theta)^{-1}f'(U(\theta,\phi|\Theta,\Phi))\partial_\Phi U(\theta,\phi|\Theta,\Phi) \\ &= A^{-1}(\sin\Theta)^{-1}\partial_\Phi f(U(\theta,\phi|\Theta,\Phi)).\end{aligned} \tag{3.19b}$$

Now substituting $\mathcal{V}_r$ into Eq. (3.11a) with h given by Eq. (2.36) for $h_0 = 0$, we have

$$\begin{aligned}H_r(\Theta,\Phi) = \bar{h}\int_{S^2} &\mathcal{V}_r(\theta,\phi|\Theta,\Phi) \\ &\times \left(\cos\bar{\theta}\cos\theta + \sin\bar{\theta}\sin\theta\cos(\phi-\bar{\phi})\right)\mathcal{D}(\theta,\phi).\end{aligned} \tag{3.20}$$

It is useful to rewrite the integrals using the $\mathbb{R}^3$ embedding (2.17):

$$H_r(\Theta,\Phi) = \bar{h}\int_{S^2} f'(U(\theta,\phi|\Theta,\Phi))\,[R(\Theta,\Phi)\mathbf{e}_r\cdot\mathbf{x}]\,[\bar{\mathbf{x}}\cdot\mathbf{x}]\mathcal{D}(\theta,\phi), \tag{3.21}$$

where $R(\Theta,\Phi) = R_3(\Phi)R_2(\Theta)$,

$$\mathbf{x} = (\sin\theta\cos\phi, \sin\theta\sin\phi, \cos\theta)^\top,$$

$$\bar{\mathbf{x}} = (\sin\bar{\theta}\cos\bar{\phi}, \sin\bar{\theta}\sin\bar{\phi}, \cos\bar{\theta})^\top.$$

Performing the change of variable $\mathbf{x}' = R(\Theta,\Phi)^{-1}\mathbf{x}$, using invariance of the dot product under rotations, and $\gamma\circ U(z|Z) = U(z|Z)$, we have

$$\begin{aligned}H_r &= \bar{h}\int_{S^2} f'(U(\theta',\phi'|\Theta,\Phi))\left[R(\Theta,\Phi)\mathbf{e}_r\cdot R(\Theta,\Phi)\mathbf{x}'\right] \\ &\quad\times [\bar{\mathbf{x}}\cdot R(\Theta,\Phi)\mathbf{x}']\mathcal{D}(\theta',\phi'), \\ &= \bar{h}\int_{S^2} f'(U(\theta',\phi'|0,0))\left[\mathbf{e}_r\cdot\mathbf{x}'\right][R(\Theta,\Phi)^{-1}\bar{\mathbf{x}}\cdot\mathbf{x}']\mathcal{D}(\theta',\phi') \\ &= \bar{h}\sum_{j=1}^3 M_{rj}(0,0)F_j(\Theta,\Phi),\end{aligned}$$

with the F_j defined according to

$$R(\Theta,\Phi)^{-1}\bar{\mathbf{x}} = (F_1(\Theta,\Phi), F_2(\Theta,\Phi), F_3(\Theta,\Phi))^\top, \tag{3.22}$$

such that $F_1^2 + F_2^2 + F_3^2 = 1$. From properties of the matrix $\mathbf{M}(0,0)$, it follows that

$$H_r = \frac{\bar{h}}{\bar{J}}F_r(\Theta,\Phi), \quad r = 1, 2. \tag{3.23}$$

Next, Eqs. (3.11b), (3.11c), (3.19) and the identity $U(\theta',\phi'|0,0) = A\cos\theta'$ imply that

$$\begin{aligned}\Gamma_1 &= A\int_{S^2} f'(U(\theta,\phi|\Theta,\Phi))\,[R(\Theta,\Phi)\mathbf{e}_1\cdot\mathbf{x}] \\ &\quad\times [R(\Theta,\Phi)\mathbf{e}_1\cdot\mathbf{x}]\,\mathcal{D}(\theta,\phi), \\ &= A\int_{S^2} f'(U(\theta',\phi'|0,0))\left[\mathbf{e}_1\cdot\mathbf{x}'\right]\left[\mathbf{e}_1\cdot\mathbf{x}'\right]\mathcal{D}(\theta',\phi') \\ &= A\mathcal{I}_0[\sin^2\theta\cos^2\phi] = A/\bar{J},\end{aligned}$$

$$\begin{aligned}\Lambda_2 &= A\sin\Theta\int_{S^2} f'(U(\theta,\phi|\Theta,\Phi))\,[R(\Theta,\Phi)\mathbf{e}_2\cdot\mathbf{x}] \\ &\quad\times [R(\Theta,\Phi)\mathbf{e}_2\cdot\mathbf{x}]\,\mathcal{D}(\theta,\phi), \\ &= A\sin\Theta\int_{S^2} f'(U(\theta',\phi'|0,0))\left[\mathbf{e}_2\cdot\mathbf{x}'\right]\left[\mathbf{e}_2\cdot\mathbf{x}'\right]\mathcal{D}(\theta',\phi') \\ &= A\sin\Theta\mathcal{I}_0[\sin^2\theta\cos^2\phi] = A\sin\Theta/\bar{J},\end{aligned}$$

$$\begin{aligned}\Gamma_2 = \Lambda_1/\sin\Theta &= A\int_{S^2} f'(U(\theta,\phi|\Theta,\Phi)) \\ &\quad\times [R(\Theta,\Phi)\mathbf{e}_2\cdot\mathbf{x}]\,[R(\Theta,\Phi)\mathbf{e}_1\cdot\mathbf{x}]\,\mathcal{D}(\theta,\phi), \\ &= A\int_{S^2} f'(U(\theta',\phi'|0,0))\left[\mathbf{e}_2\cdot\mathbf{x}'\right]\left[\mathbf{e}_1\cdot\mathbf{x}'\right]\mathcal{D}(\theta',\phi') \\ &= A\mathcal{I}_0[\sin^2\theta\sin\phi\cos\phi] = 0.\end{aligned}$$

Finally, from Eq. (3.12),

$$\begin{aligned}D_{rs} &= \int_{S^2}\int_{S^2} f'(U(\theta,\phi|\Theta,\Phi))f'(U(\theta',\phi'|\Theta,\Phi)) \\ &\quad\times [R(\Theta,\Phi)\mathbf{e}_r\cdot\mathbf{x}]\left[R(\Theta,\Phi)\mathbf{e}_s\cdot\mathbf{x}'\right] \\ &\quad\times C(\theta,\phi|\theta',\phi')\mathcal{D}(\theta,\phi)\mathcal{D}(\theta',\phi') \\ &= \int_{S^2}\int_{S^2} f'(U(\theta,\phi|0,0))f'(U(\theta',\phi'|0,0))\,[\mathbf{e}_r\cdot\mathbf{x}]\left[\mathbf{e}_s\cdot\mathbf{x}'\right] \\ &\quad\times C(\theta,\phi|\theta',\phi')\mathcal{D}(\theta,\phi)\mathcal{D}(\theta',\phi').\end{aligned} \tag{3.24}$$

It turns out that the diffusion matrix is actually diagonal, which follows from the fact that the $SO(3)$ invariant correlation function has the Karhunen–Loeve expansion (3.2). For the sake of illustration, suppose that the correlation function is expanded in terms of first-order spherical harmonics, that is, $C_1 = \bar{C}$ and $C_n = 0$ for $n \neq 1$ in Eq. (3.5):

$$C(\theta,\phi|\theta',\phi) = \bar{C}[\cos\theta\cos\theta' + \sin\theta\sin\theta'\cos(\phi-\phi')]. \tag{3.25}$$

Eq. (3.24) then simplifies into the following sum of integrals:

$$D_{rs} = \overline{C}\sum_{j=1}^{3} M_{rj}(0,0)M_{sj}(0,0),$$

where $\mathbf{M}$ is given by Eq. (2.23). That is,

$$D_{11} = \frac{\overline{C}}{\overline{J}^2} = D_{22}, \quad D_{12} = D_{21} = 0.$$

and the diffusion matrix is diagonal.

4. Analysis of stochastic phase equations

Combining the various results of Section 3, the SDEs (3.10) reduce to

$$d\Theta = \left[\sqrt{\epsilon}\frac{\bar{h}}{A}F_1(\Theta,\Phi)+O(\epsilon)\right]dt + \sqrt{2\epsilon D}dW_1(t), \tag{4.1a}$$

$$\sin\Theta d\Phi = \left[\sqrt{\epsilon}\frac{\bar{h}}{A}F_2(\Theta,\Phi)+O(\epsilon)\right]dt + \sqrt{2\epsilon D}dW_2(t). \tag{4.1b}$$

where

$$\mathbb{E}[dW_r(t)] = 0, \quad \mathbb{E}[dW_r(t)dW_s(t')] = \delta_{r,s}\delta(t-t')dt\,dt', \quad D = \frac{\overline{C}}{A^2}.$$

We have also noted the presence of $O(\epsilon)$ contributions to the drift terms, which have two distinct sources. First, the $O(d\Theta^2, d\Phi^2, d\Theta d\Phi)$ terms in Eq. (3.7) arising from Ito's lemma, which were dropped in our subsequent analysis and, second, terms that couple the amplitude and phase dynamics. If $\bar{h} > 0$ then the $O(\epsilon)$ drift terms can be ignored to a first approximation. However, as we show below, we need to include an $O(\epsilon)$ drift term when considering the diffusive wandering of a bump in the absence of an external input.

4.1. Stochastic dynamics on the sphere for $\bar{h} = 0$

In the absence of an external input, Eq. (4.1) becomes

$$\begin{aligned} d\Theta &= O(\epsilon)dt + \sqrt{2\epsilon D}dW_1(t),\\ \sin\Theta d\Phi(t) &= O(\epsilon)dt + \sqrt{2\epsilon D}dW_2(t), \end{aligned} \tag{4.2}$$

The calculation of the $O(\epsilon)$ terms is non-trivial due to the fact that the stochastic phase variables Θ, Φ couple to the amplitude v at this order of the perturbation expansion. In the case of wandering bumps on S^1 or $\mathbb{R}$, dropping these terms leads to pure Brownian motion of the bump, which is consistent with the underlying translation symmetry. On the other hand, for S^2 we will show that if the noise amplitude is $O(\sqrt{\epsilon})$ then an $O(\epsilon)$ drift term has to be included in the Θ dynamics in order to ensure that the wandering of the bump is described by Brownian motion on the sphere. The latter is necessary at the given level of approximation so that the dynamics is consistent with $SO(3)$ symmetry, and the $O(\epsilon)$ term is a direct consequence of the fact that S^2 is a curved manifold.

We begin by introducing some basic theory of stochastic differential equations on manifolds. For further details see Refs. [40–42]. We will formulate the theory for a general d-dimensional manifold $\mathcal{M}$ with metric tensor $G = [g_{ij}]$ and then consider the particular example of the sphere. Let $\mathbf{q} = (q_1,\ldots,q_d)^\top \in \mathbb{R}^d$ denote the coordinates of a patch in a d-dimensional manifold. (In the case of S^2 we can take the patch to be the largest open set $\{(\theta,\phi); 0 < \theta < \pi, 0 < \phi < 2\pi\}$.) Consider the Ito SDE

$$dq_j = A_i(\mathbf{q})dt + B_j(\mathbf{q})dW_j,$$

where the $W_j(t)$ are independent Wiener processes. Let $p(\mathbf{q},t|\mathbf{q}_0)$ denote the probability density under the initial condition $\mathbf{q}(0) = \mathbf{q}_0$ and normalization

$$\int_{\mathbb{R}^d} p(\mathbf{q},t|\mathbf{q}_0)|G(\mathbf{q})|^{1/2}d\mathbf{q} = 1,$$

where $d\mathbf{q} = dq_1\ldots dq_d$ and $DV(\mathbf{q}) = |G(\mathbf{q})|^{1/2}d\mathbf{q}$ is a volume element. Note that p satisfies the Chapman–Kolmogorov equation

$$p(\mathbf{q},t|\mathbf{q}_0) = \int_{\mathbb{R}^d} p(\mathbf{q},\tau|\mathbf{q}')p(\mathbf{q}',t-\tau|\mathbf{q}_0)|G(\mathbf{q}')|^{1/2}d\mathbf{q}'.$$

We proceed along the lines of Ref. [42] (chapter 8) by deriving the corresponding Fokker–Planck (FP) equation using a generalization of the standard derivation in $\mathbb{R}^d$ [43].

Let $\mathbf{q} = \mathbf{q}(t)$ and $\mathbf{s} = \mathbf{q}(t-dt)$. Evaluating infinitesimal moments using the SDE and Ito's lemma shows that

$$\int_{\mathbb{R}^d}(q_i - s_i)p(\mathbf{q},t|\mathbf{s})|G(\mathbf{s})|^{1/2}d\mathbf{s} = A_i(\mathbf{q},t)dt,$$

and

$$\int_{\mathbb{R}^d}(q_i - s_i)(q_j - s_j)p(\mathbf{q},t|\mathbf{s})|G(\mathbf{s})|^{1/2}d\mathbf{s} = \delta_{i,j}B_i(\mathbf{q},t)^2dt.$$

Using the Chapman–Kolmogorov equation, we have

$$\begin{aligned} \frac{\partial p(\mathbf{q},t|\mathbf{s})}{\partial t} &= \lim_{\Delta t\to 0}\frac{1}{\Delta t}[p(\mathbf{q},t+\Delta t|\mathbf{s}) - p(\mathbf{q},t|\mathbf{s})]\\ &= \lim_{\Delta t\to 0}\frac{1}{\Delta t}\\ &\quad\times\left[\int_{\mathbb{R}^d} p(\mathbf{q},t|\mathbf{q}')p(\mathbf{q}',\Delta t|\mathbf{s})|G(\mathbf{q}')|^{1/2}d\mathbf{q}' - p(\mathbf{q},t|\mathbf{s})\right]. \end{aligned}$$

Let $\psi(\mathbf{q})$ be an arbitrary compactly supported smooth function, and consider the integral equation

$$\begin{aligned} &\int_{\mathbb{R}^d}\psi(\mathbf{s})\frac{\partial p(\mathbf{q},t|\mathbf{s})}{\partial t}|G(\mathbf{s})|^{1/2}d\mathbf{s}\\ &= \lim_{\Delta t\to 0}\frac{1}{\Delta t}\left[\int_{\mathbb{R}^d}\psi(\mathbf{s})|G(\mathbf{s})|^{1/2}d\mathbf{s}\right.\\ &\quad\times\int_{\mathbb{R}^d} p(\mathbf{q},t|\mathbf{q}')p(\mathbf{q}',\Delta t|\mathbf{s})|G(\mathbf{q}')|^{1/2}d\mathbf{q}'\\ &\quad\left.-\int_{\mathbb{R}^d}\psi(\mathbf{s})p(\mathbf{q},t|\mathbf{s})|G(\mathbf{s})|^{1/2}d\mathbf{s}\right]. \end{aligned}$$

Reversing the order of integration in the double integral on the right-hand side gives

$$\begin{aligned} &\int_{\mathbb{R}^d}\psi(\mathbf{s})\frac{\partial p(\mathbf{q},t|\mathbf{s})}{\partial t}|G(\mathbf{s})|^{1/2}d\mathbf{s}\\ &= \lim_{\Delta t\to 0}\frac{1}{\Delta t}\int_{\mathbb{R}^d} p(\mathbf{q},t|\mathbf{q}')\left[\int_{\mathbb{R}^d} p(\mathbf{q}',\Delta t|\mathbf{s})\psi(\mathbf{s})|G(\mathbf{s})|^{1/2}d\mathbf{s} - \psi(\mathbf{q}')\right]\\ &\quad\times|G(\mathbf{q}')|^{1/2}d\mathbf{q}'. \end{aligned}$$

Expanding the function $\psi(\mathbf{s})$ as a Taylor series about $\mathbf{q}'$,

$$\psi(\mathbf{s}) = \psi(\mathbf{q}') + \sum_{i=1}^{d}(s_i - q_i')\frac{\partial\psi}{\partial q_i'} + \frac{1}{2}\sum_{i,j=1}^{d}(s_i - q_i')(s_j - q_j')\frac{\partial^2\psi}{\partial q_i'\partial q_j'} + \cdots$$

substituting into the previous equation, and using the moment equations yields the following result in the limit $\Delta t \to 0$:

$$\begin{aligned} &\int_{\mathbb{R}^d}\psi(\mathbf{s})\frac{\partial p(\mathbf{q},t|\mathbf{s})}{\partial t}|G(\mathbf{s})|^{1/2}d\mathbf{s}\\ &= \int_{\mathbb{R}^d}\left[\sum_{i=1}^{d}\frac{\partial\psi}{\partial s_i}A_i(\mathbf{s},t) + \frac{1}{2}\sum_{i=1}^{d}\frac{\partial^2\psi}{\partial s_i^2}B_i(\mathbf{s})^2\right]p(\mathbf{q}|\mathbf{s},t)|G(\mathbf{s})|^{1/2}d\mathbf{s}. \end{aligned}$$

The final step is to integrate the two terms on the right-hand side by parts. Using the fact that $\psi(\mathbf{s})$ has compact support, and is

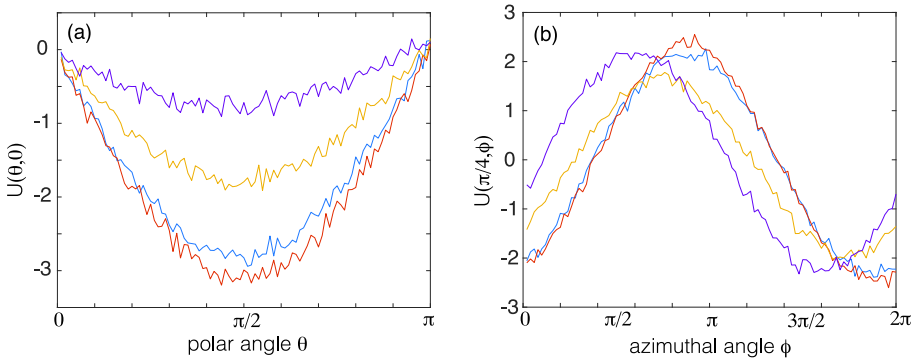

Fig. 5. Illustration of the stochastic wandering of a bump on the sphere. Snapshots of bump profile $U(\theta,\phi,t)$ at times $t = 250, 500, 750, 1000$ as a function of (a) polar angle $\theta \in [0,\pi]$ for $\phi = 0$ and (b) azimuthal angle $\phi \in [0, 2\pi]$ for $\theta = \pi/4$. The firing rate function has a gain $\eta = 4$, and a threshold $\kappa = 0.5$. Other parameter values are $J_0 = 0, \bar{J} = 1$, $\bar{h} = 0$, $\epsilon = 0.1$.

otherwise arbitrary, we obtain the FP equation

$$\frac{\partial p}{\partial t} = -|G|^{-1/2}\sum_{i=1}^{d}\frac{\partial}{\partial q_i}\left(|G|^{1/2}A_i p\right) + \frac{1}{2}|G|^{-1/2} \times \sum_{i=1}^{d}\frac{\partial^2}{\partial q_i^2}\left(|G|^{1/2}B_i^2 p\right). \tag{4.3}$$

In the case of the unit sphere S^2, the metric tensor and volume element are

$$G(\theta,\phi) = \begin{pmatrix} 1 & 0 \\ 0 & \sin^2\theta \end{pmatrix}, \quad dV = \sin\theta d\theta\, d\phi. \tag{4.4}$$

Eq. (4.3) then implies that the Fokker–Planck equation for the SDE

$$\begin{aligned} d\Theta &= A_1(\Theta,\Phi)dt + B_1(\Theta,\Phi)dW_1(t), \\ d\Phi &= A_2(\Theta,\Phi)dt + B_2(\Theta,\Phi)dW_2(t) \end{aligned} \tag{4.5}$$

is

$$\frac{\partial p}{\partial t} = -\frac{1}{\sin\Theta}\frac{\partial}{\partial\Theta}\left(\sin\Theta A_1(\Theta,\Phi)p\right) - \frac{\partial}{\partial\Phi}\left(A_2(\Theta,\Phi)p\right) + \frac{1}{2\sin\Theta}\frac{\partial^2}{\partial\Theta^2}\left(\sin\Theta B_1(\Theta,\Phi)^2 p\right) + \frac{1}{2}\frac{\partial^2}{\partial\Phi^2}\left(B_2(\Theta,\Phi)^2 p\right). \tag{4.6}$$

It can be seen that the FP equation (4.6) is equivalent to the standard diffusion equation written in spherical polar coordinates,

$$\frac{\partial p}{\partial t} = \frac{\epsilon D}{\sin\Theta}\left[\frac{\partial}{\partial\Theta}\sin\Theta\frac{\partial p}{\partial\Theta} + \frac{1}{\sin\Theta}\frac{\partial^2 p}{\partial\Phi^2}\right], \tag{4.7}$$

provided that

$$A_1 = \epsilon D\cot\Theta, \quad A_2 = 0, \quad B_1 = \sqrt{2\epsilon D}, \quad B_2 = \frac{\sqrt{2\epsilon D}}{\sin\Theta}.$$

In other words, the SDE for Brownian motion on the sphere is [44]

$$d\Theta = \epsilon D\cot\Theta dt + \sqrt{2\epsilon D}dW_1, \quad d\Phi = \frac{\sqrt{2\epsilon D}}{\sin\Theta}dW_2, \tag{4.8}$$

that is, we need to include an $O(\epsilon)$ drift term in the SDE 4.1 for $d\Theta$. This then ensures that the steady state density for the location of a wandering bump is uniform on the sphere, since the solution to Eq. (4.7) satisfies $\lim_{t\to\infty} p(\Theta,\Phi,t) = 1/4\pi$.

In Figs. 5 and 6 we show example plots of a wandering bump in a spherical attractor network. It can be seen that in the presence of noise, the neural field can be characterized by fast fluctuations of the bump profile together with a discernible shift in the position of the peak, consistent with the original decomposition (3.6). For the given example, the bump appears symmetric about $\theta = \pi/2$. Other realizations would exhibit different behavior.

4.2. Linear noise approximation for $\bar{h} > 0$

The analysis of the full stochastic equation (4.1) is considerably more involved. Here we simplify the problem using a linear noise approximation. Suppose that (Θ^*,Φ^*) is a fixed point of the deterministic dynamics obtained when $D = 0$, that is, $F_1(\Theta^*,\Phi^*) = F_2(\Theta^*,\Phi^*) = 0$. Using Eq. (3.22) and $R(\Theta,\Phi) = R_3(\Phi)R_2(\Theta)$, we have

$$R(\Theta^*,\Phi^*)^{-1}\bar{\mathbf{x}} = \pm\mathbf{e}_3,$$

which can be rewritten as

$$(\sin\bar\theta\cos\bar\phi, \sin\bar\theta\sin\bar\phi, \cos\bar\theta) = \pm\,(\sin\Theta^*\cos\Phi^*, \sin\Theta^*\sin\Phi^*, \cos\Theta^*).$$

There are thus two fixed points given by

$$(\Theta^*,\Phi^*) = Z_s^* := (\bar\theta,\bar\phi) \text{ and } (\Theta^*,\Phi^*) = Z_u^* := (\pi-\bar\theta,\pi+\bar\phi) \tag{4.9}$$

The first fixed point turns out to be stable, whereas the second is unstable, consistent with the expected result that the marginally stable bump solution can lock to a weakly biased external stimulus. That is, the peaks of the bump and input coincide: $(\Theta^*,\Phi^*) = (\bar\theta,\bar\phi)$, see also Fig. 4.

Stability of a fixed point can be determined from the eigenvalues of the Jacobian $\mathbf{N}$, which has entries

$$N_{11} = \left.\frac{\partial F_1(\Theta,\Phi)}{\partial\Theta}\right|_{\Theta=\Theta^*,\Phi=\Phi^*}, \quad N_{12} = \left.\frac{\partial F_1(\Theta,\Phi)}{\partial\Phi}\right|_{\Theta=\Theta^*,\Phi=\Phi^*}$$

$$N_{21} = \left.\frac{\partial F_2(\Theta,\Phi)/\sin\Theta}{\partial\Theta}\right|_{\Theta=\Theta^*,\Phi=\Phi^*} = \frac{1}{\sin\Theta^*}\left.\frac{\partial F_2(\Theta,\Phi)}{\partial\Theta}\right|_{\Theta=\Theta^*,\Phi=\Phi^*},$$

$$N_{22} = \frac{1}{\sin\Theta^*}\left.\frac{\partial F_2(\Theta,\Phi)}{\partial\Phi}\right|_{\Theta=\Theta^*,\Phi=\Phi^*}.$$

We have used the fact that $F_2(\Theta^*,\Phi^*) = 0$. In order to avoid the coordinate singularities at the poles, we will assume that $0 < \Theta^* < \pi$. (These singularities are simply an artifact of the choice of parameterization of the sphere, and are not physical singularities.) We will determine the first derivatives by differentiating equation (3.22) with respect to Θ and Φ, after rewriting

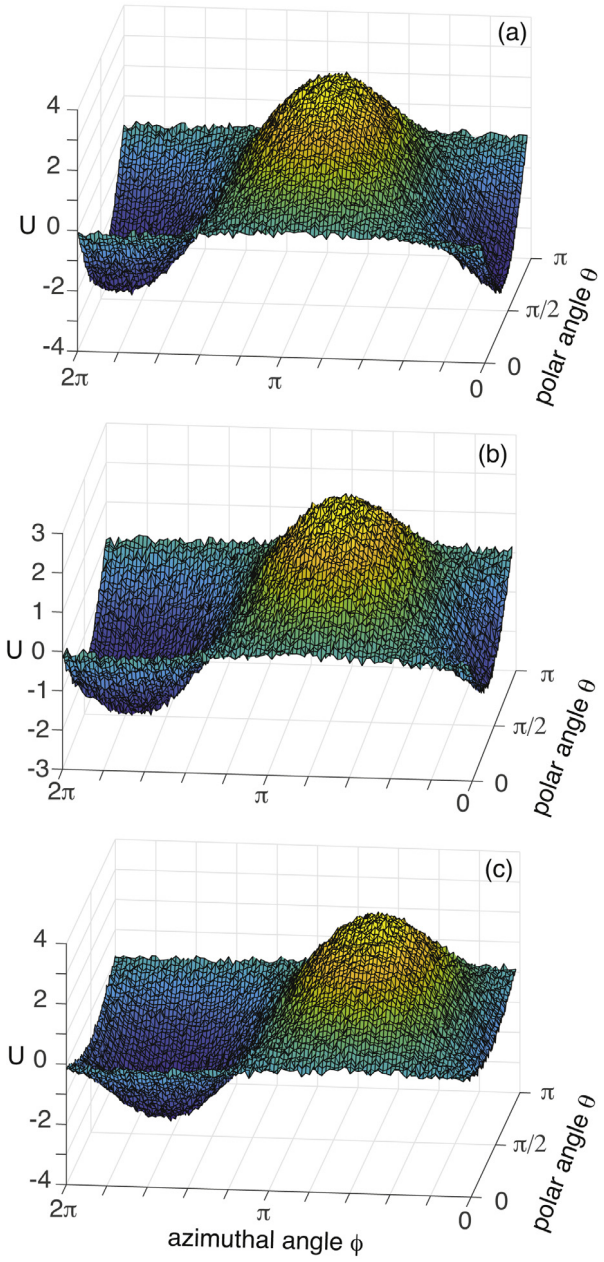

Fig. 6. Surface plots of $U(\theta,\phi,t)$ at times $t = 500, 750, 1000$, respectively. Parameter values as in Fig. 5.

it in the form

$$\bar{\mathbf{x}} = R_3(\Phi)R_2(\Theta)(F_1(\Theta,\Phi),F_2(\Theta,\Phi),F_3(\Theta,\Phi))^\top,$$

with

$$F_3 = \pm\sqrt{1-F_1^2-F_2^2},$$

corresponding to (Θ,Φ) being in a neighborhood of the fixed points Z_s^* and Z_u^*, respectively. First, we have

$$\begin{aligned}0 &= R_3(\Phi^*)R_2'(\Theta^*)(0,0,\pm1)^\top\\ &\quad + R_3(\Phi)R_2(\Theta)\frac{\partial}{\partial\Theta}(F_1(\Theta^*,\Phi^*),F_2(\Theta^*,\Phi^*),F_3(\Theta^*,\Phi^*))^\top\\ &= \begin{pmatrix}\cos\Theta^*\cos\Phi^*\\ \cos\Theta^*\sin\Phi^*\\ -\sin\Theta^*\end{pmatrix}\\ &\quad + \begin{pmatrix}\partial_\Theta F_1\cos\Theta^*\cos\Phi^* - \partial_\Theta F_2\sin\Phi^*\\ \partial_\Theta F_1\cos\Theta^*\sin\Phi^* + \partial_\Theta F_2\cos\Phi^*\\ -\partial_\Theta F_1\sin\Theta^*\end{pmatrix}.\end{aligned}$$

Note that $\partial_\Theta F_3(\Theta^*,\Phi^*)=0$. Similarly, we have

$$\begin{aligned}0 &= R_3'(\Phi^*)R_2(\Theta^*)(0,0,\pm1)^\top\\ &\quad + R_3(\Phi)R_2(\Theta)\frac{\partial}{\partial\Phi}(F_1(\Theta^*,\Phi^*),F_2(\Theta^*,\Phi^*),F_3(\Theta^*,\Phi^*))^\top\\ &= \begin{pmatrix}-\sin\Theta^*\sin\Phi^*\\ \sin\Theta^*\cos\Phi^*\\ 0\end{pmatrix}\\ &\quad + \begin{pmatrix}\partial_\Phi F_1\cos\Theta^*\cos\Phi^* - \partial_\Phi F_2\sin\Phi^*\\ \partial_\Phi F_1\cos\Theta^*\sin\Phi^* + \partial_\Phi F_2\cos\Phi^*\\ -\partial_\Phi F_1\sin\Theta^*\end{pmatrix}.\end{aligned}$$

We deduce that

$$\mathbf{N} = \begin{pmatrix}-1 & 0\\ 0 & -1\end{pmatrix}, \tag{4.10}$$

for Z_s^* and

$$\mathbf{N} = \begin{pmatrix}-1 & 0\\ 0 & 1\end{pmatrix}, \tag{4.11}$$

for Z_u^*. It follows that Z_s^* is stable and Z_u^* is unstable.

Returning to the SDE (4.1), we linearize about the stable fixed point and set

$$\sqrt{\epsilon}Y_1(t) = \Theta(t)-\Theta^*, \quad \sqrt{\epsilon}Y_2(t) = \Phi(t)-\Phi^*.$$

This yields the pair of SDEs

$$dY_1 = -\frac{\sqrt{\epsilon}\bar{h}}{A}Y_1(t)dt + \sqrt{2D}dW_1(t), \tag{4.12a}$$

$$\begin{aligned}dY_2 &= -\frac{\sqrt{\epsilon}\bar{h}}{A}Y_2(t)dt\\ &\quad + \sqrt{2D}\left(\frac{1}{\sin\Theta^*} - \frac{\cos\Theta*}{\sin^2\Theta^*}\sqrt{\epsilon}Y_1(t)\right)dW_2(t).\end{aligned} \tag{4.12b}$$

For the sake of illustration, suppose that $\Theta^* = \bar{\theta} = \pi/2$, that is, the input has a peak at the equator of the sphere. In this special case, $Y_1(t)$ and $Y_2(t)$ evolve according to a pair of identical, independent Ornstein–Uhlenbeck (OU) processes. The Fokker–Planck (FP) equation for an OU process on $\mathbb{R}$ with decay rate $\lambda = \sqrt{\epsilon}\bar{h}/A$ and diffusion coefficient D is [43]

$$\frac{\partial p(y,t)}{\partial t} = \frac{\partial[\lambda y p(y,t)]}{\partial y} + D\frac{\partial^2 p(y,t)}{\partial y^2}. \tag{4.13}$$

Given an initial condition $p(y,0)=\delta(y-y_0)$, the solution to the FP equation is a Gaussian with time-dependent mean and variance:

$$p(y,t) = \frac{1}{\sqrt{2\pi D[1-\mathrm{e}^{-2\lambda t}]/\lambda}}\exp\left(-\frac{(y-y_0\mathrm{e}^{-\lambda t})^2}{2D[1-\mathrm{e}^{-2\lambda t}]/\lambda}\right). \tag{4.14}$$

The mean and variance of the OU process are therefore given by

$$\langle Y(t)\rangle = y_0\mathrm{e}^{-\lambda t}, \quad \langle[Y(t)-\langle Y(t)\rangle]^2\rangle = \frac{D}{\lambda}(1-\mathrm{e}^{-2\lambda t}) \tag{4.15}$$

In the large time limit, we obtain a stationary Gaussian process with zero mean and time-independent variance

$$\langle Y(t)\rangle = 0, \quad \langle[Y(t)-\langle Y(t)\rangle]^2\rangle = \frac{D}{\lambda}. \tag{4.16}$$

It is important to note, however, that the linearized SDE is basically defined in the tangent plane to the sphere, $Y_r(t)\in\mathbb{R}$, and thus neglects the fact that the dynamics occurs on the surface of a sphere. The validity of the linear noise approximation will then depend on how small the width of the Gaussian densities

for Θ and Φ is compared to the inverse Gaussian curvature of the sphere. That is, we require $\epsilon D/\lambda = \sqrt{\epsilon \bar{C}}/(\bar{h}A) \ll 1$.

5. Discussion

In this paper we extended the theory of wandering bumps in stochastic neural fields to the case of a spherical network topology. This is a non-trivial extension due to the non-abelian nature of the underlying symmetry group $SO(3)$ and the fact that S^2 is a curved manifold. Using a combination of group theoretic and perturbation methods we established the following main results: (i) the wandering of a bump in the absence of an external input is characterized by Brownian motion on the sphere; (ii) the stochastic dynamics in response to a weakly biased external input can be approximated by an Ornstein–Uhlenbeck process, provided that the variance is sufficiently small so that the curvature of the sphere can be ignored.

The mathematical framework developed in this paper could be used to explore various applications of stochastic spherical attractor networks, along analogous lines to ring attractor networks. For example, if one interprets the neural field on a sphere as a model of orientation and spatial frequency tuning in a cortical hypercolumn of V1, then one natural extension would be to consider the effects of inter-network coupling between a pair of spherical attractor networks. The latter could represent populations of cells in two different layers of a cortical hypercolumn linked via vertical synaptic connections, or two different cortical hypercolumns linked by horizontal patchy connections within the same layer. As previously shown for ring attractor networks, weak inter-network coupling leads to additional terms in the SDEs for wandering bumps that can reduce the effects of noise [9,22,31]. Another extension would be to develop a more detailed model of the laminar structure of cortex. To a first approximation, cortical layers can be grouped into an input layer 4, superficial layers 2/3 and deep layers 5/6 [45,46]. The various layers can be distinguished by the source of afferents into the layer and the targets of efferents leaving the layer, the nature and extent of intralaminar connections, the identity of interneurons within and between layers, and the degree of stimulus specificity of pyramidal cells. In previous work, we explored the role of cortical layers in the propagation of waves of orientation selectivity across V1 [47], under the assumption that deep layers are less tuned to orientation. This suggests also considering coupled spherical networks that differ in their tuning properties.

From a mathematical perspective, one outstanding issue is developing a more rigorous derivation of the stochastic phase dynamics for wandering bumps on a sphere, in which the $O(\epsilon)$ coupling between the amplitude and phases is explicitly taken into account. One way to proceed would be to extend the variational approach to analyzing waves and bumps in stochastic neural fields on flat manifolds such as $\mathbb{R}$ and S^1 [28,29]. The basic idea is to minimize the error term v in the decomposition of Eq. (3.6) with respect to an appropriately defined weighted norm in the Hilbert space $L^2(S^2,\rho)$. That is, the inner product is defined according to

$$\langle u, v\rangle_\rho = \int_{S^2} u(\theta,\phi)v(\theta,\phi)\rho(\theta,\phi)\mathcal{D}(\theta,\phi), \quad u, v \in L^2(S^2,\rho),$$

where fixing ρ is the additional mathematical constraint necessary to uniquely specify the amplitude–phase decomposition (3.6), and is determined by ensuring that the error term involves fast transverse fluctuations. One of the potential advantages of the variational approach is that it can be used to derive rigorous bounds on the expected time of transverse fluctuations to escape a neighborhood of the bump solution; such a rare event leads to a break down of the perturbation construction.

Acknowledgments

P.C.B. was supported by the National Science Foundation, USA (Grant DMS-1613048).

Appendix. The special orthogonal group $SO(3)$

Lie groups

An important class of transformations is the group of invertible linear transformations in n dimensions, which can be represented by $n \times n$ real matrices A with $\det(A) \neq 0$. These form the general linear group $GL(n,R)$, which has n^2 parameters. The orthogonal group in n dimensions, $O(n)$, consists of the subset of transformations in $GL(n,R)$ that leave the Euclidean norm $\sum_{j=1}^n x_j^2$ on $\mathbb{R}^n$ invariant. It follows that $O(n)$ consists of orthogonal matrices A with the property that $A^\top = A^{-1}$. For a matrix in a neighborhood of the identity, $I+\epsilon X$, this property requires that X be skew-symmetric: $X_{ij} = -X_{ji}$. Since skew-symmetric matrices have $n(n-1)/2$ independent entries, it follows that the parameter space of $O(n)$ is also $n(n-1)/2$-dimensional. The identity

$$1 = \det(A^\top A) = \det(A^\top)\det(A)$$

implies that $\det(A) = \pm 1$. The subset of orthogonal matrices with $\det(A) = +1$ constitutes a subgroup of $O(n)$ known as the special orthogonal group $SO(n)$.

Note that $GL(n,R)$ and $O(n)$ are examples of a Lie group — a group that is also a smooth manifold in which the group operations of multiplication and inversion are smooth maps. In more detail, suppose that G is a continuous group whose elements $A \in G$ depend on N real parameters, $A = A(a)$ with $a = (a_1, \ldots, a_N)$. Under multiplication of two elements, we have

$$A(a)A(b) = A(c),$$

where c must be a continuous function of a and b: $c = f(a,b)$. Associativity of the composition law of a group,

$$A(a)[A(b)A(c)] = [A(a)A(b)]A(c),$$

means that

$$f[a, f(b,c)] = f[f(a,b), c].$$

The existence of an identity element I with $I = A(0)$ and

$$A(0)A(a) = A(a)A(0) = A(a),$$

implies that

$$f(0,a) = f(a,0) = a.$$

Finally, the existence of an inverse element $A(a)^{-1}$ with $A(a)^{-1} = A(a^*)$ and

$$A(a^*)A(a) = A(a)A(a*) = A(0),$$

shows that

$$f(a^*, a) = f(a, a^*) = 0.$$

A continuous group is said to be a Lie group if f is an analytic function, that is, a function with a Taylor series expansion within the domain defined by the parameters. We can then treat the parameters as the coordinates of an N-dimensional differentiable manifold known as the group manifold. In the case of $O(n)$, all entries of $A \in O(n)$ are bounded, $|A_{ij}| \leq 1$, so that the $n(n-1)/2$ group manifold is compact.

Lie algebras

One of the most useful objects in the study of Lie groups is the corresponding Lie algebra of infinitesimal generators. We will discuss this within the context of a matrix group G, whose corresponding Lie algebra is denoted by g. First, any element close to the identity can be written as

$$A(\epsilon a) = I + \epsilon \sum_{i=1}^{N} a_i X_i, \quad X_i = \left. \frac{\partial A(a)}{\partial a_i} \right|_{a=0},$$

where I is the identity element, $N = n(n-1)/2$, and the infinitesimal generators X_i form a basis set of vectors for the Lie algebra. (One can also view elements of the Lie algebra as vectors lying in the tangent space at the origin of the group manifold.) The composition law of the Lie group imposes a set of commutation relations for the matrices X_i:

$$[X_i, X_j] := X_i X_j - X_j X_i = c_{ij}^k X_k,$$

where the c_{ij}^k are known as the structure constants of the algebra. At a more abstract level, we can think of the commutator as a binary operation $[\cdot,\cdot] : g \times g \to g$ that satisfies the following axioms:

1. Bilinearity,
$$[\lambda_1 X + \lambda_2 Y, Z] = \lambda_1 [X, Z] + \lambda_2 [Y, Z], \; [Z, \lambda_1 X + \lambda_2 Y] = \lambda_1 [Z, X] + \lambda_2 [Z, Y]$$
for all scalars λ_1, λ_2 and all elements $X, Y, Z \in o(n)$.
2. $[X, X] = 0$
3. The Jacobi identity
$$[X, [Y, Z]] + [Z, [X, Y]] + [Y, [Z, X]] = 0$$
for all $X, Y, Z \in g$.

The first two axioms imply anti-commutativity, that is, $[X, Y] = -[Y, X]$. (For more general Lie algebras, the bilinear operation is known as a Lie bracket and need not be in the form of a commutator. However, it obeys the same axioms.) It turns out that the dimension of a Lie group and much of its structure can be understood by considering elements in a neighborhood of the identity element and carrying out computations in the Lie algebra, which are typically easier than working with the group. Intuitively speaking, any finite group transformation can be constructed by repeated application of infinitesimal transformations.

Representations of SO(3)

Let us now focus on the group $SO(3)$, whose natural representation is the matrix rotation group acting in the vector space $\mathbb{R}^3$. We will denote the Cartesian coordinates of $\mathbb{R}^3$ by the triplet (x, y, z). The most common ways to choose the three free parameters of $SO(3)$ are as follows: (i) Successive rotations about three mutually orthogonal fixed axes; (ii) Successive rotations about the z-axis, about the new y-axis, and then about the new z-axis (Euler angles); (iii) The axis–angle representation, which is defined in terms of an axis whose direction is specified by a unit vector (two parameters) and a rotation about the given axis (one parameter). We will follow the first parameterization here. The matrices corresponding to rotations about the x-axis, y-axis and z-axis are, respectively

$$R_1(\varphi_1) = \begin{pmatrix} 1 & 0 & 0 \\ 0 & \cos\varphi_1 & -\sin\varphi_1 \\ 0 & \sin\varphi_1 & \cos\varphi_1 \end{pmatrix} \tag{A.1a}$$

$$R_2(\varphi_y) = \begin{pmatrix} \cos\varphi_2 & 0 & \sin\varphi_2 \\ 0 & 1 & 0 \\ -\sin\varphi_2 & 0 & \cos\varphi_2 \end{pmatrix} \tag{A.1b}$$

$$R_3(\varphi_3) = \begin{pmatrix} \cos\varphi_3 & -\sin\varphi_3 & 0 \\ \sin\varphi_3 & \cos\varphi_3 & 0 \\ 0 & 0 & 1 \end{pmatrix} \tag{A.1c}$$

The corresponding infinitesimal generators are given by

$$X_1 = \left. \frac{\partial R_1(\varphi)}{\partial \varphi} \right|_{\phi=0} = \begin{pmatrix} 0 & 0 & 0 \\ 0 & 0 & -1 \\ 0 & 1 & 0 \end{pmatrix} \tag{A.2a}$$

$$X_2 = \left. \frac{\partial R_2(\varphi)}{\partial \varphi} \right|_{\phi=0} = \begin{pmatrix} 0 & 0 & 1 \\ 0 & 0 & 0 \\ -1 & 0 & 0 \end{pmatrix} \tag{A.2b}$$

$$X_3 = \left. \frac{\partial R_3(\varphi)}{\partial \varphi} \right|_{\phi=0} = \begin{pmatrix} 0 & -1 & 0 \\ 1 & 0 & 0 \\ 0 & 0 & 0 \end{pmatrix} \tag{A.2c}$$

From standard matrix multiplication, it follows that the commutators of the Lie algebra generated by X_1, X_2, X_3 are given by

$$[X_1, X_2] = X_3, \quad [X_2, X_3] = X_1 \quad [X_3, X_1] = X_2. \tag{A.3}$$

An alternative representation of $SO(3)$ can be obtained by considering the effect of a rotation on the unit sphere S^2 given by the equation $x^2 + y^2 + z^2 = 1$. If we introduce the spherical polar coordinates

$$x = \sin\theta\cos\phi, \quad y = \sin\theta\sin\phi, \quad z = \cos\theta, \tag{A.4}$$

then the action of any group element is to map $(\theta, \phi) \mapsto (\theta', \phi')$. Note that the sphere S^2 is a manifold rather than a vector space, so the action of $SO(3)$ on the sphere is distinct from the action of $SO(3)$ on the vector space $\mathbb{R}^3$. It is also important to distinguish between the two-dimensional manifold S^2 on which $SO(3)$ acts, and the three-dimensional manifold of the Lie group itself.

One can also consider the action of $SO(3)$ on infinite-dimensional vector space such as $L^2(\mathbb{R}^3)$. Let $\gamma \in SO(3)$ and define the induced action on functions:

$$\gamma \circ F(\mathbf{x}) = F(\gamma^{-1}\mathbf{x}), \tag{A.5}$$

where $\mathbf{x} = (x, y, z) \in \mathbb{R}^3$. Close to the identity element, we can write

$$\gamma^{-1}\mathbf{x} = (1 - \sum_{j=1,2,3} \varphi_j X_j)\mathbf{x} = \begin{pmatrix} 1 & \varphi_3 & -\varphi_2 \\ -\varphi_3 & 1 & \varphi_1 \\ \varphi_2 & -\varphi_1 & 1 \end{pmatrix} \mathbf{x},$$

which means that

$$\gamma \circ F(x, y, x) = F(x + \varphi_3 y - \varphi_2 z, y - \varphi_3 x + \varphi_1 z, z + \varphi_2 x - \varphi_1 y).$$

Assuming that F is differentiable, we can Taylor expand the right-hand side to first order in φ_i, which yields the following expression:

$$\begin{aligned} \gamma \circ F(x, y, x) &= F(x, y, z) + \varphi_1 \left(z \frac{\partial F}{\partial y} - y \frac{\partial F}{\partial z} \right) \\ &+ \varphi_2 \left(x \frac{\partial F}{\partial z} - z \frac{\partial F}{\partial x} \right) \\ &+ \varphi_3 \left(y \frac{\partial F}{\partial x} - x \frac{\partial F}{\partial y} \right) \\ &= \left(1 + \sum_{j=1}^{3} \varphi_j X_j \right) F(x, y, z), \end{aligned}$$

where X_j are now given by the differential operators

$$X_1 = z\frac{\partial}{\partial y} - y\frac{\partial}{\partial z}, \quad X_2 = x\frac{\partial}{\partial z} - z\frac{\partial}{\partial x}, \quad X_3 = y\frac{\partial}{\partial x} - x\frac{\partial}{\partial y}. \tag{A.6}$$

Note that the linear operators obey the same commutation relations (A.3). Finally, we can use the action of $SO(3)$ transformations on functions $F(x, y, z)$ to determine the corresponding infinitesimal operators acting on smooth functions in $L^2(S^2)$, which are defined on the surface of the unit sphere with angular coordinates (θ, ϕ). It can be shown that the infinitesimal generators acting on functions $F(\theta, \phi)$ take the form of Eq. (2.32), that is,

$$X_1 = \sin\phi \frac{\partial}{\partial\theta} + \frac{\cos\theta\cos\phi}{\sin\theta}\frac{\partial}{\partial\phi},$$
$$X_2 = \cos\phi \frac{\partial}{\partial\theta} - \frac{\cos\theta\sin\phi}{\sin\theta}\frac{\partial}{\partial\phi}, \quad X_3 = \frac{\partial}{\partial\phi}.$$

The question then arises whether there are finite-dimensional subspaces of $L^2(S^2)$ that are invariant under $SO(3)$, that is, they provide finite-dimensional representations of SO(3). Suppose that such a subspace V exists and is spanned by the basis set $\{f_i, i = 1, \ldots, N\}$. The subspace is invariant if and only if

$$\gamma \circ \sum_{j=1} \alpha_j f_j = \sum_{i=1}^{N} \beta_i f_i,$$

for real coefficients α_j, β_i. Linearity of the map implies that

$$b_i = \sum_{j=1}^{N} A_{ij}\alpha_j,$$

for some matrix A corresponding to an element of $SO(3)$. The vector subspace V is said to be an irreducible representation of $SO(3)$ if V contains no finite-dimensional subspaces invariant under $SO(3)$. It can be shown that every irreducible subspace is characterized by an integer $l \geq 0$ and has dimension $2l + 1$. The basic functions are given by spherical harmonics: $\{Y_{lm}, m = -l, \ldots, l\}$.

References

[1] D.C. Somers, S. Nelson, M. Sur, An emergent model of orientation selectivity in cat visual cortical simple cells, J. Neurosci. 15 (1995) 5448–5465.
[2] R. Ben-Yishai, R.L. Bar, H. Sompolinsky, Theory of orientation tuning in visual cortex, Proc. Natl. Acad. Sci. 92 (1995) 3844–3848.
[3] R. Ben-Yishai, D. Hansel, H. Sompolinsky, Traveling waves and the processing of weakly tuned inputs in a cortical network module, J. Comput. Neurosci. 4 (1997) 57–77.
[4] P.C. Bressloff, J.D. Cowan, An amplitude approach to contextual effects in primary visual cortex, Neural Comput. 14 (2002) 493–525.
[5] M. Camperi, X.J. Wang, A model of visuospatial short-term memory in prefrontal cortex: recurrent network and cellular bistability, J. Comput. Neurosci. 5 (1998) 383–405.
[6] K. Zhang, Representation of spatial orientation by the intrinsic dynamics of the head-direction cell ensemble: a theory, J. Neurosci. 16 (1996) 2112–2126.
[7] A. Compte, N. Brunel, P.S. Goldman-Rakic, X.-J. Wang, Synaptic mechanisms and network dynamics underlying spatial working memory in a cortical network model, Cerebral Cortex 10 (2000) 910–923.
[8] C.R. Laing, W.C. Troy, B. Gutkin, G.B. Ermentrout, Multiple bumps in a neuronal model of working memory, SIAM J. Appl. Math. 63 (2002) 62–97.
[9] Z.P. Kilpatrick, Inter-areal coupling reduces encoding variability in multi-area models of spatial working memory, Front. Comput. Neurosci. 7 (2013) 82.
[10] Z.P. Kilpatrick, Delay stabilizes stochastic motion of bumps in laminar neural fields, Physica D 295–296 (2015) 30–45.
[11] Z.P. Kilpatrick, Synaptic mechanisms of interference in working memory, Sci. Rep. 8 (2018) 7879.
[12] P.C. Bressloff, J.D. Cowan, An $SO(3)$ symmetry breaking mechanism for orientation and spatial frequency tuning in visual cortex, Phys. Rev. Lett. 88 (2002) 078102.
[13] P.C. Bressloff, J.D. Cowan, Spherical model of orientation and spatial frequency tuning in a cortical hypercolumn, Phil. Trans. R. Soc. B 358 (2003) 1643–1667.
[14] M. Hübener, D. Shoham, A. Grinvald, T. Bonhoeffer, Spatial relationships among three columnar systems in cat area 17, J. Neurosci. 17 (1997) 9270–9284.
[15] N.P. Issa, C. Trepel, M.P. Stryker, Spatial frequency maps in cat visual cortex, J. Neurosci. 20 (2000) 8504–8514.
[16] I. Nauhaus, K.J. Nielsen, A.A. Disney, E.M. Callaway, Orthogonal micro-organization of orientation and spatial frequency in primate primary visual cortex, Nat. Neurosci. 15 (2012) 1683–1692.
[17] G. Singh, F. Memoli, T. Ishkhanov, G. Sapiro, G. Carlsson, D.L. Ringach, Topological analysis of population activity in visual cortex, J. Vis. 8 (2008) 1–18.
[18] P.L. Nunez, R. Srinivasan, Electric Fields of the Brain: The Neurophysics of EEG, second ed., Oxford University Press, New York, 2005.
[19] S. Visser, R. Nicks, O. Faugeras, S. Coombes, Standing and travelling waves in a spherical brain model: The Nunez model revisited, Physica D 349 (2017) 27–45.
[20] C.R. Laing, C.C. Chow, Stationary bumps in networks of spiking neurons, Neural Comput. 13 (2001) 1473–1494.
[21] C.C. Chow, S. Coombes, Existence and wandering of bumps in a spiking neural network model, SIAM J. Appl. Dyn. Syst. 5 (2006) 552–574.
[22] Z.P. Kilpatrick, G.B. Ermentrout, Wandering bumps in stochastic neural fields, SIAM J. Appl. Dyn. Syst. 12 (2013) 61–94.
[23] P.C. Bressloff, M.A. Webber, Front propagation in stochastic neural fields., SIAM J. Appl. Dyn. Syst. 11 (2012) 708–740.
[24] M. Webber, P.C. Bressloff, The effects of noise on binocular rivalry waves: a stochastic neural field model, J. Stat. Mech. 3 (2013) P03001.
[25] Z.P. Kilpatrick, G.B. Ermentrout, B. Doiron, Optimizing working memory with heterogeneity of recurrent cortical excitation, J. Neurosci. 33 (2013) 18999–19011.
[26] Z.P. Kilpatrick, Coupling layers regularizes wave propagation in stochastic neural fields, Phys. Rev. E 89 (2014) 022706.
[27] P.C. Bressloff, Z.P. Kilpatrick, Nonlinear Langevin equations for the wandering of fronts in stochastic neural fields, SIAM J. Appl. Dyn. Syst. 14 (2015) 305–334.
[28] J. Inglis, J. MacLaurin, A general framework for stochastic traveling waves and patterns, with application to neural field equations, SIAM J. Appl. Dyn. Syst. 15 (2016) 195–234.
[29] P.C. Bressloff, J.N. Maclaurin, Wandering bumps and stimulus-dependent variability in a stochastic neural field: a variational approach, Preprint, 2019.
[30] A. Ponce-Alvarez, A. Thiele, T.D. Albright, G.R. Stoner, G. Devo, Stimulus-dependent variability and noise correlations in cortical MT neurons, Proc. Natl. Acad. Sci. USA 110 (2013) 13162–13167.
[31] P.C. Bressloff, Stochastic neural field model of stimulus-dependent variability in cortical neurons, PLoS Comput. Biol. (2019) In press.
[32] B. Hall, Lie Groups, Lie Algebras, and Representations: An Elementary Introduction, second ed., Springer, 2015.
[33] M. Golubitsky, I. Stewart, The Symmetry Perspective: From Equilibrium to Chaos in Phase Space and Physical Space, Birkhauser, Basel, 2002.
[34] R. Hoyle, Pattern Formation: An Introduction to Methods, Cambridge University Press, Cambridge, 2006.
[35] P.C. Bressloff, Spatiotemporal dynamics of continuum neural fields, J. Phys. A 45 (2012) 033001, Invited topical review.
[36] G. Arfken, Mathematical Methods for Physicists, third ed., Academic Press, San Diego, 1985.
[37] O. Faugeras, Inglis. J., Stochastic neural field theory: a rigorous footing, J. Math. Biol. 71 (2014) 259–300.
[38] M. Kruger, W. Stannat, Front propagation in stochastic neural fields: a rigorous mathematical framework, SIAM J. Appl. Dyn. Syst. 13 (2014) 1293–1310.
[39] A. Lang, C. Schwab, Isotropic Gaussian random fields on the sphere: regularity, fast simulation and stochastic partial differential equations, Anal. Appl. Probab. 25 (2015) 3047–3094.
[40] R.W. Brockett, Notes on stochastic processes on manifolds, in: C.I. Byrnes, et al. (Eds.), Systems and Control in the Twenty-First Century, Birkhauser, Boston, 1997.
[41] E.P. Hsu, Stochastic Analysis on Manifolds, in: Graduate Studies in Mathematics, vol. 38, American Mathematical Society, Providence, RI, 2002.
[42] G.S. Chirikjian, Stochastic Models, Information Theory, and Lie Groups, Volume 1: Classical Results and Geometric Methods, Birkhauser, Boston, 2009.
[43] C.W. Gardiner, Handbook of Stochastic Methods, fourth ed., Springer, Berlin, 2009.
[44] D.R. Brillinger, A particle migrating randomly on a sphere, J. Theor. Probab. 10 (1997) 429–443.
[45] E.M. Callaway, Local circuits in primary visual cortex of the macaque monkey, Ann. Rev. Neurosci. 121 (1998) 47–74.
[46] J.A. Hirsch, L.M. Martinez, Laminar processing in the visual cortical column, Curr. Opin. Neurobiol. 16 (2006) 377–384.
[47] P.C. Bressloff, S.R. Carroll, Laminar neural field model of laterally propagating waves of orientation selectivity, PLoS Comput. Biol. 11 (10) (2015) e1004545.